Multilevel Preconditioning of Discontinuous–Galerkin Spectral Element Methods Part I: Geometrically Conforming Meshes

Kolja Brix[*], **Martin Campos Pinto**[§¶],
Claudio Canuto[||] and **Wolfgang Dahmen**[*]

Bericht Nr. 355 **Januar 2013**

Key words: Discontinuous Galerkin discretization for elliptic problems, interior penalty method, locally refined meshes, variable polynomial degrees, auxiliary space method, Gauß–Lobatto grids, dyadic grids.

AMS Subject Classifications: 65N35, 65N55, 65N30, 65N22, 65F10, 65F08

Institut für Geometrie und Praktische Mathematik
RWTH Aachen

Templergraben 55, D–52056 Aachen (Germany)

---

* Institut für Geometrie und Praktische Mathematik, RWTH Aachen, Templergraben 55, 52056 Aachen, Germany, e–mail: `{brix,dahmen}@igpm.rwth-aachen.de`

§ CNRS, UMR 7598, Laboratoire Jacques–Louis Lions, 4 Place Jussieu, F–75005, Paris, France

¶ UPMC Univ Paris 06, UMR 7598, Laboratoire Jacques–Louis Lions, 4 Place Jussieu, F–75005, Paris, France, e–mail: `campos@ann.jussieu.fr`

|| Dipartimento di Scienze Matematiche, Politecnico di Torino, Corso Duga degli Abruzzi 24, 10129 Torino, Italy, e–mail: `claudio.canuto@polito.it`

This work was supported in part by the European Commission Improving Human Potential Programme within project "Breaking Complexity" (HPRN–CT–2002–00286), by the RWTH Aachen Seed Funds project funded by the Excellence Initiative of the German federal and state governments, and by DFG project "Optimal preconditioners of spectral Discontinuous Galerkin methods for elliptic boundary value problems" (DA 117/23-1).

Multilevel Preconditioning of Discontinuous-Galerkin Spectral Element Methods Part I: Geometrically Conforming Meshes

Kolja Brix[*], Martin Campos Pinto[§,¶], Claudio Canuto[‖] and Wolfgang Dahmen[*]

January 28, 2013

Abstract This paper is concerned with the design, analysis and implementation of preconditioning concepts for spectral DG discretizations of elliptic boundary value problems. The far term goal is to obtain robust solvers for the "fully flexible" case. By this we mean Discontinuous Galerkin schemes on locally refined quadrilateral or hexahedral partitions with hanging nodes and variable polynomial degrees that could, in principle, be arbitrarily large only subject to some weak grading constraints. In this paper, as a first step, we focus on varying arbitrarily large degrees while keeping the mesh geometrically conforming since this will be seen to exhibit already some essential obstructions. The conceptual foundation of the envisaged preconditioners is the auxiliary space method, or in fact, an iterated variant of it. The main conceptual pillars that will be shown in this framework to yield "optimal" preconditioners are Legendre-Gauß-Lobatto grids in connection with certain associated anisotropic nested dyadic grids. Here "optimal" means that the preconditioned systems exhibit uniformly bounded condition numbers. Moreover, the preconditioners have a modular form that facilitates somewhat simplified partial realizations at the expense of a moderate loss of efficiency. Our analysis is complemented by careful quantitative experimental studies of the main components.

AMS subject classification 65N35, 65N55, 65N30, 65N22, 65F10, 65F08

Keywords Discontinuous Galerkin discretization for elliptic problems, interior penalty method, locally refined meshes, variable polynomial degrees, auxiliary space method, Gauß-Lobatto grids, dyadic grids.

1 Introduction

Attractive features of discontinuous Galerkin (DG) discretizations are on one hand their versatility regarding a variety of different problem types as well as on the other hand their flexibility regarding local mesh refinement and even locally varying the order of the discretization. While initially the main focus has been on transport problems like hyperbolic conservation laws an increased attention has recently been paid to diffusion problems which naturally enter the picture in more complex applications like the compressible or incompressible Navier-Stokes equations. Well-posedness and stability issues are by now fairly well understood [4, 3] although these studies refer primarily to

[*]Institut für Geometrie und Praktische Mathematik, RWTH Aachen, Templergraben 55, 52056 Aachen, Germany, e–mail: {brix,dahmen}@igpm.rwth-aachen.de

[§]CNRS, UMR 7598, Laboratoire Jacques-Louis Lions, 4 Place Jussieu, F-75005, Paris, France

[¶]UPMC Univ Paris 06, UMR 7598, Laboratoire Jacques-Louis Lions, 4 Place Jussieu, F-75005, Paris, France, e–mail: campos@ann.jussieu.fr

[‖]Dipartimento di Scienze Matematiche, Politecnico di Torino, Corso Duca degli Abruzzi 24, 10129 Torino, Italy, e–mail: claudio.canuto@polito.it.

This work was supported in part by the European Commission Improving Human Potential Programme within project "Breaking Complexity" (HPRN-CT-2002-00286), by the RWTH Aachen Seed Funds project funded by the Excellence Initiative of the German federal and state governments, and by DFG project "Optimal preconditioners of spectral Discontinuous Galerkin methods for elliptic boundary value problems" (DA 117/23-1).

uniform fixed degrees and conforming domain partitions, see, e.g., [11, 12] for locally refined meshes and variable degrees.

Of course, the option of choosing very high polynomial degrees is of particular interest for diffusion problems since under certain circumstances highly regular, even analytic solutions occur that are best treated by spectral discretizations [15]. The fact that in most practical situations a very high regularity is encountered only in part of the domain has led to the concept of *hp*-discretizations which typically come about as conforming methods. However, the DG framework seems to be particularly well suited for accommodating strongly varying polynomial degrees (see, e.g., [24, 26]) in combination with local mesh refinements admitting hanging nodes.

While stability of such discretizations can be ensured, as will be seen below, essentially following standard lines, the issue of efficiently solving the resulting linear systems of equations seems to be much less clear. For quasi-uniform meshes and uniform (low) polynomial degrees a multigrid scheme, proposed in [18], (covering actually convection-diffusion problems as well) does give rise to uniformly bounded condition numbers for diffusive problems provided that (i) the underlying hierarchy of meshes is *quasi-uniform* and (ii) the solution exhibits a certain (weak) regularity. This scheme has been extended in [19] to locally refined meshes showing a similar performance without a theoretical underpinning though. Domain decomposition preconditioners investigated in [1, 2], give rise to only moderately growing condition numbers. A two-level scheme in the sense of the *auxiliary space method* (see, e.g., [7, 22, 28]) has been proposed in [17] and shown to exhibit mesh-independent convergence again on quasi-uniform conforming meshes with a fixed uniform polynomial degree. In the framework of the auxiliary space method preconditioners providing uniformly bounded condition numbers for locally refined meshes under weak grading constraints and variable but uniformly bounded polynomial degrees have been developed in [11, 12], but again the results are valid only for a fixed bound on the polynomial degrees with constants depending on that bound.

The state of the art concerning preconditioners that are robust with respect to the polynomial degrees is somewhat heterogeneous. Meanwhile a fairly good understanding has been developed for pure spectral discretizations, i.e. for a single polynomial patch [15, 14, 23, 6]. In the DG context the current results seem to draw primarily from domain decomposition concepts, see, e.g., [25]. To our knowledge they are subject to two type of constraints, namely to geometrically conforming meshes and to uniform poynomial degrees p. The best known results seem to offer bounds on condition numbers of only logarithmic growth in p.

The objective of this paper is therefore to develop and analyze preconditioners for what we call *Spectral-Element-DG* discretizations, eventually exploiting the full flexibility potential of the DG concept, meaning arbitrarily large varying polynomial degrees and local refinements with hanging nodes, both only subject to mild grading constraints. The central theoretical challenge hings on the question how to design preconditioners that give rise to *uniformly bounded* condition numbers in the most flexible setting described above. We shall address this challenge in the context of the auxiliary space method [22, 27, 28]. However, to keep the paper at an acceptable length, as a first step we confine the discussion here on *geometrically conforming* meshes, i.e., hanging nodes are avoided but varying polynomial degrees of arbitrary size are permitted. In fact, some essential obstructions are already encountered in this case for the following reason. First, on the basis of the experience in the context of spectral methods, in our opinion the most promising avenue towards fully robust preconditioners with respect to polynomial degrees is to employ concepts centering around *Legendre-Gauß-Lobatto grids* (LGL-grids). As soon as the degrees on adjacent polynomial patches differ the corresponding LGL-grids do not match at the patch interfaces (the more so when dealing with hanging nodes) since LGL-grids are *not* nested. This turns out to have far reaching consequences in several respects, namely properly dealing with jump terms on the patch interfaces but also regarding the efficient solution of the patchwise problems in case of very large degrees. One of the remedies we propose is to employ auxiliary spaces based on certain anisotropic dyadic grids which are associated with the LGL-grids but which in addition are nested. Therefore, the concepts developed for the geometrically conforming case will be similarly relevant in the general case as well.

Aside from these principal theoretical issues the second main theme of the present studies is to explore the quantitative performance of the main building blocks entering such preconditioners.

The layout of the paper is as follows. After formulating in Sect. 2 our model problem and the basic ingredients concerning Legendre-Gauß-Lobatto (LGL)-grids, we recall in Sect. 3 the relevant conditions of the auxiliary space method. Sect. 4 offers a brief orientation concerning the subsequent development of a two-stage preconditioner. The first stage, using high-order conforming polynomials as auxiliary space is treated in Sect. 5. As a preparation of the subsequent second stage we discuss in Sect. 6 a major ingredient of our approach, namely certain hierarchies of nested dyadic grids associated with LGL-grids in a way that mutual interpolation between low order finite elements on these grids is stable in L_2 and H^1. Based on these findings we develop and analyze in Sect. 7 stage II of our preconditioner where the new auxiliary spaces are built by low-order finite elements on dyadic grids. We conclude in Sect. 8 with detailed numerical studies of the various ingredients of the preconditioner to assess its quantitative performance in dependence of the various parameters entering the scheme. In particular, in Sect. 8.3.1 we discuss efficient ways of applying the "relaxation" operator defined by the auxiliary space method.

Throughout the paper we shall employ the following notational convention. By $a \lesssim b$ we mean that the quantity a can be bounded by fixed constant multiple of b, independent on the parameters a and b may depend on. Likewise $a \simeq b$ means $a \lesssim b$ and $b \lesssim a$.

2 Formulation of SE-DG schemes

In this section, we introduce the basic high-order DG discretization of a second-order model problem, as well as several variants of it. We start by recalling some essential concepts about Legendre methods and Legendre Gauß-Lobatto grids on a single Cartesian element.

2.1 (Hyper-)rectangles, polynomial spaces and LGL grids

Let $I = [a, b]$ be any bounded interval, of size $H = b - a$. For any fixed integer $p \geq 1$, let $\mathbb{P}_p(I)$ be the space of the restrictions to I of the algebraic polynomials of degree $\leq p$ on the real line. Let $a = \xi_0 < \cdots < \xi_{j-1} < \xi_j < \cdots < \xi_p = b$ be the Legendre-Gauß-Lobatto (LGL) quadrature nodes of order p in I, for which there exist weights $w_0 < \cdots < w_{j-1} < w_j < \cdots < w_p$ such that

$$\sum_{j=0}^{p} v(\xi_j)\, w_j = \int_I v(x)\, dx \qquad \forall v \in \mathbb{P}_{2p-1}(I)\ . \tag{2.1}$$

We will denote by $\mathcal{G}_p(I)$ the set of such nodes, which will be referred to as the LGL grid in I. Obviously, any $v \in \mathbb{P}_p(I)$ is uniquely determined by its values on $\mathcal{G}_p(I)$. We recall that nodes and weights are classically defined on the reference interval $\hat{I} = [-1, 1]$, as $\hat{\xi}_j$, $\hat{w}_j$, resp.. By affine transformation, one has $\xi_j = a + H(\hat{\xi}_j + 1)/2$ and $w_j = (H/2)\hat{w}_j$. We also recall that weights with index j close to 0 or p satisfy $w_j \simeq Hp^{-2}$ (in particular, $w_0 = w_p = H(p(p+1))^{-1}$), whereas weights with index j close to $p/2$ satisfy $w_j \simeq Hp^{-1}$. Yet, the variation in the order of magnitude is smooth, as made precise by the estimates

$$1 \lesssim \min_{1\leq j\leq p} \frac{w_{j-1}}{w_j} \ \leq\ \max_{1\leq j\leq p} \frac{w_{j-1}}{w_j} \lesssim 1\ , \tag{2.2}$$

which hold uniformly in j, p and H (see, e.g., [13, 23]). A fundamental property for the sequel (see, e.g., [15]) is that the bilinear form

$$(u, v)_{0,I,p} = \sum_{j=0}^{p} u(\xi_j) v(\xi_j)\, w_j \tag{2.3}$$

is an inner product in $\mathbb{P}_p(I)$, which induces therein a norm uniformly equivalent to the L^2-norm:

$$\|v\|_{0,I} \le \|v\|_{0,I,p} \le \sqrt{3}\|v\|_{0,I} \qquad \forall v \in \mathbb{P}_p(I) \ . \tag{2.4}$$

Furthermore, we shall make frequent use of the following "trace" inequality: for any $v \in \mathbb{P}_p(I)$, one has

$$|v(e)| \le \frac{p+1}{\sqrt{H}} \, \|v\|_{0,I} \ , \tag{2.5}$$

where $e \in \{a, b\}$ denotes any endpoint of I. This follows, by a scaling argument, from the expansion $v(x) = \sum_{k=0}^{p} \hat{v}_k L_k(x)$ in Legendre orthogonal polynomials on the reference interval $\hat{I}$, using the Cauchy-Schwarz inequality together with the properties $|L_k(\pm 1)| = 1$ and $\|L_k\|^2_{0,\hat{I}} = 2/(2k+1)$.

Another useful property will be a refined version of the classical inverse inequality $\|v'\|_{0,I} \lesssim \dfrac{p^2}{H} \, \|v\|_{0,I}$ which holds for all $v \in \mathbb{P}_p(I)$, and reads as follows:

$$\|v'\|_{0,I} \lesssim \left(\sum_{j=0}^{p} v^2(\xi_j) w_j^{-1} \right)^{1/2} \qquad \forall v \in \mathbb{P}_p(I) \ . \tag{2.6}$$

A proof will be given in Sect. 6.

Next, let $d \ge 1$ denote the space dimension of interest. Given d bounded intervals I_k, $1 \le k \le d$, of size H_k and carrying polynomials of degree p_k, we form the corresponding d-tuples $p = (p_1, \ldots, p_d)$ and $H = (H_1, \ldots, H_d)$, we define the tensor-product space of polynomials of degree up to p_k in the k-th coordinate on the (hyper-)rectangle $R = \times_{k=1}^{d} I_k$ as

$$\mathbb{Q}_p(R) = \bigotimes_{k=1}^{d} \mathbb{P}_{p_k}(I_k) \ . \tag{2.7}$$

Occasionally, we write $p = p(R)$ and $H = H(R)$.

Given any integer $0 \le l \le d$, let $\mathcal{F}_l(R)$ denote the set of all l-dimensional facets of R, i.e., the subsets of ∂R obtained by freezing $d-l$ coordinates to one of the endpoint values of the corresponding intervals. Thus, $\mathcal{F}_0(R)$ is the set of the 2^d vertices of R, $\mathcal{F}_{d-1}(R)$ is the set of all faces of R, whereas $\mathcal{F}_d(R) = \{R\}$. Obviously, if $v \in \mathbb{Q}_p(R)$ and $F \in \mathcal{F}_l(R)$ for some $1 \le l \le d$, then $v_{|F} \in \mathbb{Q}_{p_*}(F)$, where $p_* = p_*(F)$ is obtained from p by dropping the components corresponding to the frozen coordinates.

Polynomials in $\mathbb{Q}_p(R)$ are uniquely determined through their values at the tensorial LGL-grid in R

$$\mathcal{G}_p(R) = \bigtimes_{k=1}^{d} \mathcal{G}_{p_k}(I_k) = \{\xi = (\xi_{1,j_1}, \xi_{2,j_2}, \ldots, \xi_{d,j_d}) \quad \text{for} \ \ 0 \le j_k \le p_k, \quad 1 \le k \le d\} \ , \tag{2.8}$$

where the ξ_{k,j_k} are the nodes of the LGL quadrature formula of order p_k in I_k. Introducing the product weight $w_\xi = w_{1,j_1} w_{2,j_2} \cdots w_{d,j_d}$ associated to each node $\xi \in \mathcal{G}_p(R)$, we obtain the quadrature formula

$$\sum_{\xi \in \mathcal{G}_p(R)} v(\xi) \, w_\xi = \int_R v(x) \, dx \qquad \forall v \in \mathbb{Q}_p(R) \ . \tag{2.9}$$

Then, the discrete inner product in $\mathbb{Q}_p(R)$

$$(u, v)_{0,R,p} = \sum_{\xi \in \mathcal{G}_p(R)} u(\xi) v(\xi) \, w_\xi \tag{2.10}$$

defines a norm which, thanks to (2.4), is uniformly equivalent to the L^2-norm, i.e.,

$$\|v\|_{0,R} \le \|v\|_{0,R,p} \le \left(\sqrt{3}\right)^d \|v\|_{0,R} \qquad \forall v \in \mathbb{Q}_p(R) \ . \tag{2.11}$$

LGL-grids as well as discrete inner products and norms restrict to any facet of R in the obvious way, yielding objects with analogous properties (see Sect. 5.1 for more details).

Finally, applying the bound (2.5) and tensorizing in the remaining directions, we easily get the following "trace inequality", which will be crucial in the analysis of the DG discretization.

Property 2.1. *Let $F \in \mathcal{F}_{d-1}(R)$ be a face of R, orthogonal to the k-th direction, for some $1 \leq k \leq d$. Then,*

$$\|v\|_{0,F} \leq \frac{p_k + 1}{\sqrt{H_k}} \|v\|_{0,R} \qquad \forall v \in \mathbb{Q}_p(R) \ . \tag{2.12}$$

2.2 Model problem and discretizations

We formulate now various versions of what we call *Spectral-Element Discontinuous-Galerkin* (SE-DG) discretizations for second order boundary value problems. In principle, the developments presented below apply under fairly weak assumptions on the problem parameters. To keep the technical level of the exposition as low as possible we confine the discussion to the model problem

$$-\Delta u = f \quad \text{in } \Omega \ , \qquad u = 0 \quad \text{on } \partial\Omega \ , \tag{2.13}$$

where $\Omega \subset \mathbb{R}^d$, $d \geq 2$, is a bounded Lipschitz domain with piecewise smooth boundary and $f \in L^2(\Omega)$. Such domains can be partitioned into images of (hyper-)rectangles through smooth mappings (such as iso/sub-parametric mappings, or Gordon-Hall transforms). Again, in order to keep technicalities at a possibly low level, it suffices to treat unions of (hyper-)rectangles, i.e., we assume that the closure of Ω can be partitioned into the union of a finite collection $\mathcal{R}$ of (hyper-)rectangles R, which overlap at most through parts of their boundaries. Precisely, in this paper we will consider only *geometrically conforming partitions* $\mathcal{R}$, characterized by the fact that any nonempty intersection between two elements R and R' in $\mathcal{R}$ is an l-facet for both of them, for some $0 \leq l \leq d-1$. An example of a 2D conforming patch of elements is given in Fig. 1. It will be convenient to introduce the complex

$$\mathcal{F}_l := \bigcup_{R \in \mathcal{R}} \mathcal{F}_l(R)$$

of all l-dimensional faces associated with the macro-mesh consisting of the elements $R \in \mathcal{R}$.

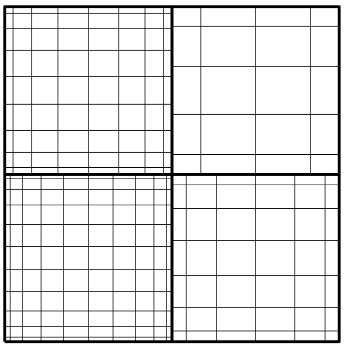

Figure 1: A geometrically conforming patch of elements in $\mathbb{R}^2$, with the corresponding LGL-grids

Recall from Sect. 2.1 that the k-th component of the vector $H = H(R) \in \mathbb{R}^d_+$ is the k-th side length of R. Likewise $p = p(R) \in \mathbb{N}^d$ denotes the vector of coordinatewise polynomial degrees of an element of $\mathbb{Q}_p(R)$. The vector-valued, piecewise constant functions H and p are thus defined throughout Ω forming the function $\delta = (H, p)$ which collects the approximation parameters for the chosen DG-SE discretization.

We assume the aspect ratios of the elements are uniformly bounded and that the distribution of polynomial degrees within each R as well as between adjacent elements R^- and R^+ is *graded* in the sense that

$$\frac{\max_k H_k(R)}{\min_k H_k(R)} \lesssim 1, \qquad \frac{\max_k p_k(R)}{\min_k p_k(R)} \lesssim 1, \qquad \max_{\pm} \max_{k} \frac{p_k(R^{\pm})}{p_k(R^{\mp})} \lesssim 1, \ \ R \in \mathcal{R}. \tag{2.14}$$

In particular, this implies that our meshes are *quasi-uniform.*

The approximation space for the DG-SE discretization is defined as

$$V_\delta = \{ v \in L^2(\Omega) \ : \ \forall R \in \mathcal{R}, \text{ there exists } v_R \in \mathbb{Q}_p(R) \text{ such that } v_{|R} = v_R \text{ a.e.} \} \ ; \tag{2.15}$$

note that any $v \in V_\delta$ can be identified with the vector of polynomial functions $(v_R)_{R\in\mathcal{R}}$.

To introduce the standard notation for DG approximations of Problem (2.13), assume that $F \in \mathcal{F}_{d-1}$ is an interior face shared by two elements which we denote by R^- and R^+. If v is a piecewise polynomial function defined on both sides of F, which takes values v^- in R^- and v^+ in R^+, then its jump $[v]_F$ across F and its average $\{v\}_F$ on F are defined as

$$[v]_F = \mathbf{n}_{R^-,F}\, v^-_{|F} + \mathbf{n}_{R^+,F}\, v^+_{|F}, \qquad \{v\}_F = \frac{1}{2}\left(v^-_{|F} + v^+_{|F} \right),$$

respectively, where $\mathbf{n}_{R^-,F} = -\mathbf{n}_{R^+,F}$ denote the unit normal vectors on F pointing to the exterior of R^-. Taking the homogeneous Dirichlet boundary condition into account, we set $[v]_F = \mathbf{n}_{R,F}\, v_{|F}$ and $\{v\}_F = v_{|F}$ when $F \subset \partial\Omega$.

Within this setting, we consider the *Symmetric Interior-Penalty Discontinuous Galerkin Spectral-Element discretization* of Problem (2.13) defined as (see [3, 4]): find $u \in V_\delta$ such that

$$a^*_\delta(u, v) = (f, v)_{0,\Omega} \quad \forall v \in V_\delta \ , \tag{2.16}$$

where the bilinear form a^*_δ on $V_\delta \times V_\delta$ is given by

$$a^*_\delta(u, v) = \sum_{R\in\mathcal{R}} (\nabla u, \nabla v)_{0,R} + \sum_{F\in\mathcal{F}_{d-1}} \Big(-(\{\nabla u\}, [v])_{0,F} - (\{\nabla v\}, [u])_{0,F} + \gamma\omega_F([u], [v])_{0,F} \Big) \ . \tag{2.17}$$

The weights ω_F are defined as follows. Assume that the interface F is orthogonal to the k-th direction. If F is shared by two elements R^- and R^+, then we set

$$\omega_F = \max\left(\frac{(p_k(R^-)+1)^2}{H_k(R^-)}, \frac{(p_k(R^+)+1)^2}{H_k(R^+)} \right) \ , \tag{2.18}$$

where the particular choice of ω_F will be justified later. On the other hand, if F is contained in $\partial\Omega$ and belongs to the element R, we set

$$\omega_F = \frac{(p_k(R)+1)^2}{H_k(R)} \ . \tag{2.19}$$

Finally, the constant $\gamma > 0$ is chosen in order to guarantee the coercivity of the bilinear form a_δ with respect to the DG-norm, defined in V_δ by

$$\|v\|^2_{DG,\delta} = \sum_{R\in\mathcal{R}} \|\nabla v\|^2_{0,R} + \gamma \sum_{F\in\mathcal{F}_{d-1}} \omega_F \|\, [v]\, \|^2_{0,F} \ . \tag{2.20}$$

Indeed, the following proposition, which is a specialization of a well-known general result about DG methods to the present situation (see, e.g., [11]), confirms the uniform continuity and coercivity of the form a^*_δ, which implies well-posedness of the discretization scheme (2.16).

Proposition 2.2. *There exists a constant $\gamma_0 > 0$ such that for all $\gamma > \gamma_0$ the bilinear form a_δ^* defined in* (2.17) *satisfies*

$$a_\delta^*(v,v) \simeq \|v\|_{DG,\delta}^2 \qquad \forall v \in V_\delta \ . \tag{2.21}$$

The constant γ_0 and the constants implied by the symbol $\simeq$ can be chosen independent of δ.

Proof. We just highlight the crucial step in the proof, which is the bound of each quantity

$$|(\{\nabla v\}, [v])_{0,F}| \leq \|\{\nabla v\}\|_{0,F} \, \| \, [v] \, \|_{0,F} \leq \frac{\eta}{2\omega_F} \|\{\nabla v\}\|_{0,F}^2 + \frac{\omega_F}{2\eta} \| \, [v] \, \|_{0,F}^2,$$

where $\eta > 0$ is a suitable weight allowing us to control these terms by the two terms appearing in the DG-norm. Assume first that F is an interior face, orthogonal to the k-th direction and shared by the two elements R^- and R^+. Then, denoting by ∂_k the partial derivative with respect to the k-th coordinate, we obtain

$$\|\{\nabla v\}\|_{0,F}^2 = \frac{1}{4} \|(\partial_k v^-)_{|F} + (\partial_k v^+)_{|F}\|_{0,F}^2 \leq \sum_{\pm} \|(\partial_k v^\pm)_{|F}\|_{0,F}^2 \leq \omega_F \sum_{\pm} \|\partial_k v^\pm\|_{0,R^\pm}^2 \ ,$$

where we have used the trace inequality (2.12). A similar estimate holds when F is a boundary face. The rest of the proof is standard. □

2.3 Numerical integration

Computational efficiency is usually enhanced, within a nodal-basis approach such as the one adopted here, by inserting high-order numerical integration (NI) into the Galerkin scheme at hand. This is accomplished by replacing the exact L^2 inner products on any element R and any face F by suitable discrete inner products based on Legendre-Gauß-Lobatto quadrature formulas. While on each element R it is enough to use the inner product defined in (2.10), some care is needed on a face F, where restrictions of polynomials of different degrees may come into play. Let us detail the latter situation.

Assume that $F \in \mathcal{F}_{d-1}$ is shared by two contiguous elements $R^\pm$, and is orthogonal to the k-th direction. Let $p_*^\pm$ be the vectors of $(d-1)$ polynomial degrees, obtained from $p^\pm = p(R^\pm)$ by deleting the k-th entries. If $v \in V_\delta$, and if $v^\pm$ denotes its restriction to $R^\pm$, then $(v^\pm)_{|F}$ belongs to $\mathbb{Q}_{p_*^\pm}(F)$. Let us introduce the vector $p_* = \max(p_*^-, p_*^+)$, where the maximum is taken component-wise. Then both $(v^-)_{|F}$ and $(v^+)_{|F}$ belong to $\mathbb{Q}_{p_*}(F)$. Thus, it makes sense to consider the $(d-1)$-dimensional LGL-grid $\mathcal{G}_{p_*}(F)$ on F corresponding to the polynomial-degree vector p_*, as well as the corresponding quadrature nodes. The induced inner product in $\mathbb{Q}_{p_*}(F)$ will be denoted by

$$(u,v)_{0,F,p_*} = \sum_{\zeta \in \mathcal{G}_{p_*}(F)} u(\zeta)\, v(\zeta)\, w_\zeta \ . \tag{2.22}$$

With these notation at hand, we assume that $f \in C^0(\overline{\Omega})$ and we obtain the modified DG-NI (Discontinuous Galerkin with Numerical Integration) scheme: find $u \in V_\delta$ such that

$$a_{\delta,\mathrm{NI}}^*(u,v) = (f,v)_{\Omega,\mathrm{NI}} \quad \forall v \in V_\delta \ , \tag{2.23}$$

where

$$\begin{aligned} a_{\delta,\mathrm{NI}}^*(u,v) =& \sum_{R \in \mathcal{R}} (\nabla u, \nabla v)_{0,R,p} \\ &+ \sum_{F \in \mathcal{F}_{d-1}} \big(-(\{\nabla u\},[v])_{0,F,p_*} - (\{\nabla v\},[u])_{0,F,p_*} + \gamma \omega_F ([u],[v])_{0,F,p_*} \big) \ , \end{aligned} \tag{2.24}$$

and

$$(f,v)_{\Omega,\mathrm{NI}} = \sum_{R\in\mathcal{R}} (f,v)_{0,R,p} \; . \tag{2.25}$$

Note that at the algebraic level, the computation of the interface terms may require suitable transfer operators between LGL-grids.

Proposition 2.2 admits a completely analogous statement for the form $a^*_{\delta,NI}$, which can be established through repeated applications of the norm equivalence (2.11) in each R and F.

2.4 The SE-DG reduced bilinear form

In view of Proposition 2.2 and its NI-counterpart, both forms a^*_δ and $a^*_{\delta,\mathrm{NI}}$ are uniformly equivalent to one of the reduced bilinear forms

$$a_\delta(u,v) = \sum_{R\in\mathcal{R}} (\nabla u, \nabla v)_{0,R} + \gamma \sum_{F\in\mathcal{F}_{d-1}} \omega_F([u],[v])_{0,F} \; , \tag{2.26}$$

or

$$a_{\delta,\mathrm{NI}}(u,v) = \sum_{R\in\mathcal{R}} (\nabla u, \nabla v)_{0,R,p} + \gamma \sum_{F\in\mathcal{F}_{d-1}} \omega_F([u],[v])_{0,F,p_*} \; . \tag{2.27}$$

Therefore, we will continue our discussion by investigating efficient preconditioners for these forms. In particular, theoretical considerations will be developed for the conceptually simpler form (2.26), although numerical results will be obtained using the complete, yet computationally more efficient form (2.24).

3 The auxiliary space method

A suitable conceptual framework for developing preconditioners for the linear system (2.16) is offered by the so called *auxiliary space method* (see, e.g., [7, 27, 28, 12]). For convenience of the reader we briefly recall now the general setting adopting the abstract framework, see [22, 20, 21].

Let V be a finite-dimensional space contained in some functional space X, and let $a : V \times V \to \mathbb{R}$ be a given symmetric positive-definite bilinear form. Let us introduce an auxiliary space $\tilde{V}$, still contained in X and finite-dimensional, which carries a symmetric positive-definite bilinear form $\tilde{a} : \tilde{V}\times\tilde{V} \to \mathbb{R}$. Let us assume that two symmetric positive-definite bilinear forms are defined on the sum $\hat{V} = V + \tilde{V}$, say $\hat{a}$, $b : \hat{V}\times\hat{V} \to \mathbb{R}$, which satisfy the following conditions:

i) $\hat{a}$ is a spectrally equivalent extension of both a and $\tilde{a}$, i.e.,

$$a(v,v) \simeq \hat{a}(v,v) \quad \forall v \in V \,, \tag{3.1}$$

$$\tilde{a}(\tilde{v},\tilde{v}) \simeq \hat{a}(\tilde{v},\tilde{v}) \quad \forall \tilde{v} \in \tilde{V} \,. \tag{3.2}$$

ii) b dominates a on V, i.e.,

$$a(v,v) \lesssim b(v,v) \quad \forall v \in V \,; \tag{3.3}$$

iii) there exist linear operators $Q : \tilde{V} \to V$ and $\tilde{Q} : V \to \tilde{V}$ such that

$$\tilde{a}(\tilde{Q}v,\tilde{Q}v) \lesssim a(v,v) \qquad \forall v \in V \;, \tag{3.4}$$

$$a(Q\tilde{v},Q\tilde{v}) \lesssim \tilde{a}(\tilde{v},\tilde{v}) \qquad \forall \tilde{v} \in \tilde{V} \;, \tag{3.5}$$

and

$$b(v-\tilde{Q}v, v-\tilde{Q}v) \lesssim \hat{a}(v,v) \qquad \forall v \in V \;, \tag{3.6}$$

$$b(\tilde{v}-Q\tilde{v}, \tilde{v}-Q\tilde{v}) \lesssim \hat{a}(\tilde{v},\tilde{v}) \qquad \forall \tilde{v} \in \tilde{V} \;. \tag{3.7}$$

Remark 3.1. *If condition ii) above is replaced with the stronger condition:*

ii') b dominates $\hat{a}$ on $\hat{V}$, i.e.,

$$\hat{a}(\hat{v},\hat{v}) \lesssim b(\hat{v},\hat{v}) \quad \forall \hat{v} \in \hat{V} \ , \tag{3.8}$$

then one can skip checking inequalities (3.4) *and* (3.5) *in iii).*

Proposition 3.2. *Under the assumptions* (3.1)*–*(3.7)*, the following norm equivalence in V holds:*

$$\hat{c}\, a(v,v) \ \leq \inf_{\substack{w \in V,\ \tilde{v} \in \tilde{V} \\ v = w + Q\tilde{v}}} \{b(w,w) + \tilde{a}(\tilde{v},\tilde{v})\} \ \leq \ \hat{C}\, a(v,v) \qquad \forall v \in V \ , \tag{3.9}$$

where the constants $\hat{c}$ and $\hat{C}$ only depend on the constants implied by the assumptions (see [9] for their expression).

Remark 3.3. *It is worth mentioning the special case when $\tilde{V}$ can be chosen as a proper subspace of V. Then $\hat{V} = V$ and natural choices for $\tilde{a}$ and $\hat{a}$ are the form a itself, whereas an obvious choice for Q is the canonical injection. In such a situation, the only assumptions that need be checked for Proposition 3.2 to hold are:*

$$a(v,v) \lesssim b(v,v) \quad \forall v \in V \tag{3.10}$$

and the existence of a linear operator $\tilde{Q} : V \to \tilde{V}$ such that

$$b(v - \tilde{Q}v, v - \tilde{Q}v) \lesssim a(v,v) \qquad \forall v \in V \ . \tag{3.11}$$

At the algebraic level, Proposition 3.2 has the following main consequence. Let $\mathbf{A}$, $\tilde{\mathbf{A}}$ and $\mathbf{B}$ denote the Gramian matrices for the bilinear forms a, $\tilde{a}$ and b (restricted to $V \times V$) with respect to suitable bases of the spaces V and $\tilde{V}$. Let $\mathbf{S}$ be the matrix representing the action of Q in these bases.

Corollary 3.4. *Under the assumptions* (3.1)*–*(3.7)*, let $\mathbf{C_B}$ and $\mathbf{C_{\tilde{A}}}$ be symmetric preconditioners for $\mathbf{B}$ and $\tilde{\mathbf{A}}$, respectively, satisfying the following spectral bounds:*

$$\lambda_{\max}(\mathbf{C_B B}),\ \lambda_{\max}(\mathbf{C_{\tilde{A}}}\tilde{\mathbf{A}}) \leq \Lambda_{\max}, \qquad \lambda_{\min}(\mathbf{C_B B}),\ \lambda_{\min}(\mathbf{C_{\tilde{A}}}\tilde{\mathbf{A}}) \geq \Lambda_{\min} \ .$$

Then, $\mathbf{C_A} = \mathbf{C_B} + \mathbf{S}\mathbf{C_{\tilde{A}}}\mathbf{S}^T$ is a symmetric preconditioner for $\mathbf{A}$, and the spectral condition number of $\mathbf{C_A A}$ satisfies

$$\kappa(\mathbf{C_A A}) \leq \frac{\Lambda_{\max}}{\Lambda_{\min}}\ \frac{\hat{C}}{\hat{c}} \ .$$

4 Orientation

We shall employ the auxiliary space method for preconditioning the linear system arising from the **SE-DG** - *Spectral-Element Discontinuous-Galerkin* discretization introduced in Sect. 2.

Perhaps a few comments on the possible choices of auxiliary spaces are in order. It has been seen in [11, 12] that for bounded polynomial degrees a low order conforming finite element subspace works well. Rougly speaking, it then sufficies to apply simple relaxation to the "nonconforming" part of the DG finite elements space and to employ multilevel preconditioning techniques to the conforming low order subspace. Since constants arising in this analysis depend on the polynomial degree in the DG-space this strategy cannot be expected to work in its original form in the present context. Instead one learns from experiences in the spectral element method (see e.g. [6, 15, 14, 23]) that suitable auxiliary spaces should be based on low order finite elements on LGL-grids, introduced in Sect. 2.1.

However, then several serious difficulties arise. The first one is rather obvious, namely how to precondition in the case of very large degrees corresponding low order finite element discretizations since the particular associated grids are not nested and typical multilevel techniques cannot be applied directly? Moreover, multilevel techniques work well, as mentioned above, when dealing with (globally) conforming discretizations. This latter issue is more subtle but turns out to pose serious obstructions as soon as one uses different polynomial degrees on different patches. Specifically, LGL-grids on adjacent patches with different polynomial degrees do not match and globally conforming subspaces are too thin for preconditioning. Therefore, it seems that an additional "second stage" auxiliary subspace is needed. For this purpose we shall construct suitable low order conforming finite element subspaces on certain *dyadically* refined (but anisotropic) grids associated with the LGL-grids, see Sect. 6, giving rise to the **DFE-CG** - *Dyadic-Finite-Element Continuous-Galerkin* schemes. These grids can be nested and thus used to form sufficiently "rich" globally conforming subspaces to which multilevel preconditioners apply.

Now the question arises "why not using the latter spaces directly as auxiliary spaces for the **SE-DG** discretizations?" Again, a second look at this option reveals that the jump terms in the DG bilinear form cause serious problems when trying to fulfill the above requirements in the auxiliary space framework. In fact, although the degrees of two adjacent polynomial patches may differ the jump across the interface could vanish since one of the traces may happen to degenerate to the common lower degree. However, since the corresponding LGL-grids do not match the respective associated dyadic grids differ as well and will therefore give rise in general to nontrivial jumps of the corresponding piecewise linears. This incompatibility of the jump terms seems to hinder the verification of the ASM conditions.

Therefore, it seems that one has to resort to an *iterated application* of the auxiliary space method. The preceeding remarks concerning the compatibility of jump terms in different discretizations suggest to reduce the problem as quickly as possible to a conforming one for which one can employ standard energy inner products. Therefore, as a first-stage auxiliary space we choose the largest conforming subspace of V_δ, referred to as **SE-CG** - *Spectral-Element Continuous-Galerkin* space. This is already interesting in its own right since it can be combined with (nearly optimal) domain decomposition preconditioners, see [16].

Since local FE spaces on contiguous elements with LGL-grids can be glued together to produce non-trivial globally conforming spaces only when the polynomial degrees are all equal, we shall use this concept only implicitly and propose to pass from **SE-CG** directly to **DFE-CG**. Once we have arrived at that stage, one can proceed to preconditioning this latter problem by suitable multilevel techniques. Due to the anisotropies of the involved dyadic grids this is, however, not quite straight forward. We develop therefore a multi-wavelet based preconditioner whose detailed elaboration is, however, deferred to the forthcoming part II of this work.

In conclusion, we propose the following route to an *iterated auxiliary space preconditioner*:

- **IAS-PATH:** **SE-DG** $\rightarrow$ **SE-CG** $\rightarrow$ **DFE-CG** .

The first stage will be discussed in Sect. 5, whereas the second one will be detailed in Sect. 7.

We proceed collecting the necessary technical prerequisites for the LGL-grids in Sect. 5.1 and for the associated dyadic grids in Sect. 6.

5 Stage SE-DG $\rightarrow$ SE-CG

In this section, we investigate the use of conforming spectral elements as auxiliary spaces. Before defining the constitutive ingredients and checking the ASM assumptions, we introduce some additional notation and we add a few remarks, which will be helpful here and throughout the remainder of the paper.

5.1 Auxiliary material

Given two integers $0 \le l, m \le d$ and a facet $F \in \mathcal{F}_l$, we set

$$\mathcal{F}_m(F) = \{G \in \mathcal{F}_m \,:\, G \subset F \text{ if } m < l \,,\; G = F \text{ if } m = l \,,\; G \supset F \text{ if } m > l\} \,. \tag{5.1}$$

In particular, $\mathcal{F}_l(R)$ has been already defined as the set of all l-facets of an element $R \in \mathcal{R}$, whereas $\mathcal{R}(F) = \mathcal{F}_d(F)$ is the set of all elements R containing the facet F.

Given any $R \in \mathcal{R}$ and the corresponding LGL-grid $\mathcal{G}_p(R)$, if $F \in \mathcal{F}_l(R)$ for some $1 \le l \le d-1$, then $\mathcal{G}_p(R) \cap F$ is the LGL-grid of the induced quadrature formula on F, which will be denoted by $\mathcal{G}_p(F,R)$. The order of the formula, denoted by $p_* = p(F,R) \in \mathbb{N}^l$, is obtained from the vector $p = p(R)$ by deleting the $d-l$ components corresponding to the frozen coordinates of F. The weights of the formula, denoted by $w_\xi^{F,R}$, are connected to the weights w_ξ of the original formula on R by the relation

$$w_\xi = w_{f_1} \cdots w_{f_{d-l}} w_\xi^{F,R} \qquad \forall \xi \in \mathcal{G}_p(F,R) \,, \tag{5.2}$$

where each w_{f_i} is a boundary weight of the univariate LGL formula along one of the frozen coordinates of F. This implies that if the facet F' belongs to $\mathcal{F}_{l-1}(F) \subset \mathcal{F}_{l-1}(R)$, then

$$w_\xi^{F',R} = w_f w_\xi^{F,R} \qquad \forall \xi \in \mathcal{G}_p(F',R) \,, \tag{5.3}$$

for some boundary weight w_f.

Next, let us draw some consequences from the assumptions (2.14) of quasi-uniformity of the mesh and polynomial degree grading. Under these assumptions, it is easily seen that given any $R \in \mathcal{R}$, there exists a real $\mathsf{H} = \mathsf{H}_R > 0$ and an integer $\mathsf{p} = \mathsf{p}_R > 0$, such that for all $R' \in \mathcal{R}$ satisfying $R' \cap R \neq \emptyset$, it holds

$$H_k(R') \simeq \mathsf{H}_R \,, \qquad p_k(R') \simeq \mathsf{p}_R \,, \qquad 1 \le k \le d \,, \tag{5.4}$$

i.e., lengths and degrees are locally comparable. More generally, for any face $F \in \mathcal{F}_l$, $l < d$, one can define analogous "representative parameters" $\mathsf{H}_F, \mathsf{p}_F$, for instance, by averaging corresponding parameters from intersecting faces. This implies, on the one hand, that each boundary weight w_j, $j \in \{0, p_k(R')\}$ of any univariate LGL formula used in the definition of the tensorial LGL formula on R' satisfies

$$w_j \simeq \frac{\mathsf{H}}{\mathsf{p}^2} \,, \tag{5.5}$$

and, on the other hand, that each face $F \in \mathcal{F}_{d-1}(R')$ carries a DG weight ω_F satisfying

$$\omega_F \simeq \frac{\mathsf{p}^2}{\mathsf{H}} \,. \tag{5.6}$$

In particular, all the faces $F \in \mathcal{F}_{d-1}$ having a nonempty intersection with an element R carry weights ω_F of comparable size.

5.2 Definition of the ASM ingredients

Referring to the notation of Sect. 3, let us choose as V the space V_δ introduced in (2.15), whereas as $\tilde{V}$ we choose the space $\tilde{V}_\delta = V_\delta \cap H_0^1(\Omega)$. Since $\tilde{V} \subset V$, Remark 3.3 applies, and we are only required to define two bilinear forms $a, b \,:\, V \times V \to \mathbb{R}$ and a linear operator $\tilde{Q} \,:\, V \to \tilde{V}$ for which conditions (3.10) and (3.11) are fulfilled.

The bilinear form a will be the reduced form a_δ defined in (2.26). Note that on $\tilde{V}_\delta$ it reduces to the standard inner product in $H_0^1(\Omega)$, since

$$a_\delta(u,v) = \sum_{R \in \mathcal{R}} (\nabla u, \nabla v)_{0,R} = (\nabla u, \nabla v)_{0,\Omega} \qquad \forall u, v \in \tilde{V}_\delta \,.$$

The definition of the form b is inspired by the inverse inequality (2.6) and requires the following notation. Let $R \in \mathcal{R}$ be any element, and $\xi \in \mathcal{G}_p(R)$ be any LGL quadrature node in R, with associated weight $w_\xi = w_{j_1} w_{j_2} \cdots w_{j_d}$; we denote by $w_{\xi,k}$ the factor w_{j_k} coming from the k-th direction. Then, we introduce the weights

$$W_\xi = \left(\sum_{k=1}^{d} w_{\xi,k}^{-2} \right) w_\xi = \sum_{k=1}^{d} w_{\xi,k}^{-1} \Big(\prod_{j \neq k} w_{\xi,j} \Big) \, . \tag{5.7}$$

We also introduce strictly positive coefficients c_ξ, satisfying the requirement $c_\xi \simeq 1$ (precisely, they should be bounded from above and from below independently of ξ, p and H under the assumptions (2.14)). They will be chosen with the aim of enhancing the effects of the ASM preconditioner; we refer to Sect. 8 for the details.

Definition 5.1. *The bilinear form $b_\delta \, : \, V_\delta \times V_\delta \to \mathbb{R}$ is defined as follows:*

$$b_\delta(u,v) = \sum_{R \in \mathcal{R}} b_R(u,v) \, , \qquad \textit{with} \quad b_R(u,v) := \sum_{\xi \in \mathcal{G}_p(R)} u(\xi) \, v(\xi) \, c_\xi W_\xi \, .$$

Note that the bilinear form b_δ is defined strictly elementwise, i.e. it does not involve any coupling between different elements R, which is essential for the efficient applicability of the preconditioner $\mathbf{B}$ in Corollary 3.4.

Before giving the definition of the operator $\tilde{Q}_\delta \, : \, V_\delta \to \tilde{V}_\delta$, we introduce a new assumption on the local distribution of the polynomial degrees, which indeed poses a restriction only for $d \geq 3$.

Assumption 5.2. *For $2 \leq l \leq d-1$ and for each $F \in \mathcal{F}_l$, there exists $R \in \mathcal{R}(F)$ such that*

$$p(F,R) \leq p(F,R') \qquad \forall R' \in \mathcal{R}(F)$$

(the inequality being taken componentwise).

Note that the property is trivially true for $l = 1$ since $p(F,R) \in \mathbb{N}$, and for $l = d$ since $\mathcal{R}(F) = \{F\}$. Thus, for each $F \in \mathcal{F}_l$ with $1 \leq l \leq d$, we are entitled to select, once and for all, an element $R^\sharp(F)$ such that

$$R^\sharp(F) := \mathrm{argmin}_{R' \in \mathcal{R}(F)} p(F,R'), \qquad p^\sharp(F) := p(F, R^\sharp(F)). \tag{5.8}$$

The LGL-grid $\mathcal{G}_p(F, R^\sharp(F))$ will be denoted by $\mathcal{G}_{p^\sharp}(F)$. Finally, for each vertex $x \in \mathcal{F}_0$ of the decomposition we select an element $R^\sharp(x)$.

The definition of the operator $\tilde{Q}_\delta$ will be accomplished through a recursive procedure, as follows.

Definition 5.3. *For $0 \leq l \leq d$, set*

$$F_l = \bigcup_{F \in \mathcal{F}_l} F \, .$$

Given any $v \in V_\delta$, let us define the sequence of piecewise polynomial functions $\tilde{q}_l \, : \, F_l \to \mathbb{R}$ by the following recursion:

i) For any $x \in \mathcal{F}_0$, set $\tilde{q}_0(x) = 0$ if $x \in \partial\Omega$ and $\tilde{q}_0(x) = v_{R^\sharp(x)}(x)$ if $x \in \Omega$.

ii) For $l = 1, \ldots, d$, define $\tilde{q}_l$ on F_l as follows: for any $F \in \mathcal{F}_l$, set $\tilde{q}_{l|F} = 0$ if $F \subset \partial\Omega$, otherwise define $\tilde{q}_{l|F}$ by the conditions

$$\begin{aligned} &\tilde{q}_{l|F} \in \mathbb{Q}_{p^\sharp}(F) \ \textit{such that} \\ &\tilde{q}_{l|F}(\xi) = v_{R^\sharp(F)}(\xi) \qquad \forall \xi \in \mathcal{G}_{p^\sharp}(F) \setminus \partial_l F \, , \\ &\tilde{q}_{l|F}(\xi) = \tilde{q}_{l-1}(\xi) \qquad \forall \xi \in \mathcal{G}_{p^\sharp}(F) \cap \partial_l F \, , \end{aligned} \tag{5.9}$$

where $\partial_l F$ denotes the boundary of F as an l-dimensional manifold.

Finally, we set

$$\tilde{Q}_\delta v = \tilde{q}_d \ . \tag{5.10}$$

Remark 5.4. *The above recursion defines a linear operator $\tilde{Q}_\delta$ from V_δ into $\tilde{V}_\delta$.*

In fact, the linearity of $\tilde{Q}_\delta$ is obvious. Moreover, note that $\tilde{Q}_\delta v \in V_\delta$ since $p^\sharp(R) = p(R)$ for all $R \in \mathcal{R}$. Furthermore, one has the property

$$\tilde{q}_{l|F_{l-1}} = q_{l-1} \qquad 1 \le l \le d \ . \tag{5.11}$$

Indeed, if $F \in \mathcal{F}_l$ and $F' \in \mathcal{F}_{l-1}(F)$, then $\tilde{q}_{l|F'} \in \mathbb{Q}_{p(F',R^\sharp(F))}(F')$ whereas $\tilde{q}_{l-1|F'} \in \mathbb{Q}_{p(F',R^\sharp(F'))}(F')$. The minimality property (5.8) applied to F', together with the last set of conditions in (5.9), imply that $\tilde{q}_{l|F'} = \tilde{q}_{l-1|F'}$, whence (5.11) follows. This property implies that $\tilde{Q}_\delta v$ is continuous throughout $\overline{\Omega}$, and vanishes on $\partial\Omega$. We conclude that $\tilde{Q}_\delta v$ belongs to $\tilde{V}_\delta$.

5.3 Check of the ASM assumptions

We shall now first verify (3.10) in Remark 3.3. To this end, the following immediate consequences of (5.5) and (5.6) concerning the weights W_ξ introduced in (5.7) will be useful.

Lemma 5.5. *Let $R \in \mathcal{R}$ be arbitrary. For any face $F \in \mathcal{F}_{d-1}$ and any $\xi \in \mathcal{G}_p(F,R)$, one has*

$$W_\xi \simeq \omega_F w_\xi^{F,R} \ .$$

Proposition 5.6. *For b_δ given in Definition 5.1 one has*

$$a_\delta(v,v) \lesssim b_\delta(v,v) \qquad \forall v \in V_\delta \ .$$

Proof. For any $R \in \mathcal{R}$, using (2.3), (2.4) and (2.6) together with tensorization, one obtains

$$\|\nabla v\|_{0,R}^2 = \sum_{k=1}^d \|\partial_k v\|_{0,R}^2 \lesssim \sum_{k=1}^d \sum_{\xi \in \mathcal{G}_p(R)} v(\xi)^2\, w_{\xi,k}^{-1} \Big(\prod_{j \ne k} w_{\xi,j} \Big) = \sum_{\xi \in \mathcal{G}_p(R)} v(\xi)^2\, W_\xi \ ,$$

whence

$$\sum_{R \in \mathcal{R}} \|\nabla v\|_{0,R}^2 \lesssim b_\delta(v,v) \ .$$

On the other hand, let $F \in \mathcal{F}_{d-1}$ be a face shared by two elements, say $R^\pm$. Then, recalling the definition of $p_*^\pm$ given in Sect. 2.3, we have

$$\|\,[v]\,\|_{0,F}^2 \lesssim \sum_\pm \|v^\pm\|_{0,F}^2 \lesssim \sum_\pm \|v^\pm\|_{0,F,p_*^\pm}^2 = \sum_\pm \sum_{\xi \in \mathcal{G}_p(F,R^\pm)} (v^\pm(\xi))^2 w_\xi^{F,R^\pm} \ .$$

Multiplying by ω_F and using Lemma 5.5 for both $R = R^\pm$, we obtain

$$\omega_F \|\,[v]\,\|_{0,F}^2 \lesssim \sum_\pm \sum_{\xi \in \mathcal{G}_p(F,R^\pm)} (v^\pm(\xi))^2\, W_\xi^\pm \le \sum_\pm \sum_{\xi \in \mathcal{G}_p(R^\pm)} (v^\pm(\xi))^2\, W_\xi^\pm \ .$$

A similar result holds for the faces $F \in \mathcal{F}_{d-1}$ sitting on the boundary of Ω. Hence,

$$\sum_{F \in \mathcal{F}} \omega_F \|\,[v]\,\|_{0,F}^2 \lesssim b_\delta(v,v) \ ,$$

and the result is proven. □

We now focus on verifying assumption (3.11). This will be accomplished through a sequence of intermediate results.

Lemma 5.7. *For any $v \in V_\delta$, let its restriction to $R \in \mathcal{R}$ be denoted by v_R. The following bound holds*
$$b_\delta(v - \tilde{Q}_\delta v, v - \tilde{Q}_\delta v) \lesssim \sum_{F \in \mathcal{F}_{d-1}} \omega_F \sum_{R \in \mathcal{R}(F)} \|v_R - \tilde{q}_{d-1}\|^2_{0,F}, \quad v \in V_\delta,$$
where $\tilde{q}_{d-1}$ is constructed in Definition 5.3 in order to define $\tilde{Q}_\delta v$.

Proof. By definition of b_δ, one has
$$b_\delta(v - \tilde{Q}_\delta v, v - \tilde{Q}_\delta v) = \sum_{R \in \mathcal{R}} \sum_{\xi \in \mathcal{G}_p(R)} |(v_R - \tilde{Q}_\delta v)(\xi)|^2 \, c_\xi W_\xi \; .$$

In view of (5.10), $(\tilde{Q}_\delta v)_{|R} = \tilde{q}_{d|R}$ and $\tilde{q}_d$ coincides with v_R on $\mathcal{G}_p(R) \backslash \partial R$ and with $\tilde{q}_{d-1}$ on $\mathcal{G}_p(R) \cap \partial R$. Thus, since $c_\xi \simeq 1$
$$\begin{aligned} b_\delta(v - \tilde{Q}_\delta v, v - \tilde{Q}_\delta v) \;&\simeq\; \sum_{R \in \mathcal{R}} \sum_{\xi \in \mathcal{G}_p(R) \cap \partial R} |(v_R - \tilde{q}_{d-1})(\xi)|^2 \, W_\xi \\ &\leq\; \sum_{R \in \mathcal{R}} \sum_{F \in \mathcal{F}_{d-1}(R)} \sum_{\xi \in \mathcal{G}_p(F,R)} |(v_R - \tilde{q}_{d-1})(\xi)|^2 \, W_\xi \\ &\lesssim\; \sum_{F \in \mathcal{F}_{d-1}} \omega_F \sum_{R \in \mathcal{R}(F)} \sum_{\xi \in \mathcal{G}_p(F,R)} |(v_R - \tilde{q}_{d-1})(\xi)|^2 \, w_\xi^{F,R} \; , \end{aligned}$$
where we have used Lemma 5.5 in the last inequality. Finally, we observe that $v_{R|F} \in \mathbb{Q}_{p(F,R)}(F)$, whereas $\tilde{q}_{d-1|F} \in \mathbb{Q}_{p^\sharp(F)}(F) \subseteq \mathbb{Q}_{p(F,R)}(F)$. Thus, (2.11) yields
$$\sum_{\xi \in \mathcal{G}_p(F,R)} |(v_R - \tilde{q}_{d-1})(\xi)|^2 \, w_\xi^{F,R} \simeq \|v_R - \tilde{q}_{d-1}\|^2_{0,F}$$
proving the assertion. □

Lemma 5.8. *Let $v \in V_\delta$ be arbitrary, and let $\tilde{q}_l$, $0 \leq l \leq d$, be the sequence built in Definition 5.3 in order to define $\tilde{Q}_\delta v$. For $1 \leq l \leq d-1$, given any $F \in \mathcal{F}_l$ and any $R \in \mathcal{R}(F)$, the following bound holds*
$$\|v_R - \tilde{q}_l\|^2_{0,F} \lesssim \sum_{G \in \mathcal{F}_{d-1}(F)} \| \, [v]_G \, \|^2_{0,F} + \frac{\mathsf{H}}{\mathsf{p}^2} \sum_{F' \in \mathcal{F}_{l-1}(F)} \|v_{R^\sharp(F)} - \tilde{q}_{l-1}\|^2_{0,F'} \; , \tag{5.12}$$
where $[v]_G$ denotes the jump of v across the internal face G, or $v|_G$ when $G \subset \partial\Omega$. Here, $\mathsf{H} = \mathsf{H}_F$ and $\mathsf{p} = \mathsf{p}_F$ are representative values of the local meshsizes and polynomial degrees, introduced in (5.4)*. On the other hand, for any vertex $x \in \mathcal{F}_0$ and any $R \in \mathcal{R}(x)$, one has*
$$|(v_R - \tilde{q}_0)(x)|^2 \lesssim \sum_{G \in \mathcal{F}_{d-1}(x)} | \, [v]_G(x) \, |^2 \; . \tag{5.13}$$

Proof. Assume first $l > 0$. If $F \subset \partial R \cap \partial\Omega$, then
$$\|v_R - \tilde{q}_l\|^2_{0,F} = \|v_R\|^2_{0,F} \lesssim \sum_{G \in \mathcal{F}_{d-1}(F)} \| \, [v]_G \, \|^2_{0,F} \; ,$$
which is a particular instance of (5.12). Let us then assume $F \not\subset \partial\Omega$ and, for simplicity, let us set $R^\sharp = R^\sharp(F)$. Observe that the definition of $\tilde{q}_{l|F}$ on $\mathcal{G}_{p^\sharp}(F) \cap \partial_l F$ given in (5.9) can be rephrased as $\tilde{q}_{l|F}(\xi) = v_{R^\sharp}(\xi) + \big(\tilde{q}_{l-1}(\xi) - v_{R^\sharp}(\xi)\big)$, or equivalently,
$$\tilde{q}_{l|F} = v_{R^\sharp|F} + \sum_{\xi \in \mathcal{G}_{p^\sharp}(F) \cap \partial_l F} \big(\tilde{q}_{l-1}(\xi) - v_{R^\sharp}(\xi)\big) \psi_\xi^F \; ,$$

where $\psi_\xi^F \in \mathbb{Q}_{p^\sharp}(F)$ denotes the Lagrangean function associated with the node ξ of the LGL-grid on F of order $p^\sharp$. Thus, using once more (2.11), we obtain

$$\|v_R - \tilde{q}_l\|_{0,F}^2 \lesssim \|v_R - v_{R^\sharp}\|_{0,F}^2 + \sum_{\xi \in \mathcal{G}_{p^\sharp}(F) \cap \partial_l F} |\tilde{q}_{l-1}(\xi) - v_{R^\sharp}(\xi)|^2 w_\xi^{F,R^\sharp} =: A^2 + B^2 .$$

As for the first quantity, there exists a sequence $R^i \in \mathcal{R}(F)$, $i = 0, \dots, m \leq d-l$ such that $R^0 = R$, $R^m = R^\sharp$ and $R^{i-1} \cap R^i \in \mathcal{F}_{d-1}(F)$ for $i = 1, \dots, m$. Thus,

$$A^2 \lesssim \sum_{i=1}^m \|v_{R^i} - v_{R^{i-1}}\|_{0,F}^2 \leq \sum_{G \in \mathcal{F}_{d-1}(F)} \| [v]_G \|_{0,F}^2 .$$

On the other hand, using (5.3) and (5.5), we have

$$\begin{aligned} B^2 &\leq \sum_{F' \in \mathcal{F}_{l-1}(F)} \sum_{\xi \in \mathcal{G}_p(F',R^\sharp)} |\tilde{q}_{l-1}(\xi) - v_{R^\sharp}(\xi)|^2 w_\xi^{F,R^\sharp} \\ &\lesssim \frac{\mathsf{H}}{\mathsf{p}^2} \sum_{F' \in \mathcal{F}_{l-1}(F)} \sum_{\xi \in \mathcal{G}_p(F',R^\sharp)} |\tilde{q}_{l-1}(\xi) - v_{R^\sharp}(\xi)|^2 w_\xi^{F',R^\sharp} \simeq \frac{\mathsf{H}}{\mathsf{p}^2} \sum_{F' \in \mathcal{F}_{l-1}(F)} \|v_{R^\sharp} - \tilde{q}_{l-1}\|_{0,F'}^2 , \end{aligned}$$

where the last equivalence follows, as in the proof of the previous lemma, by observing that $v_{R^\sharp|F'} \in \mathbb{Q}_{p(F',R^\sharp)}(F')$ whereas $\tilde{q}_{l-1|F'} \in \mathbb{Q}_{p^\sharp(F')}(F') \subseteq \mathbb{Q}_{p(F',R^\sharp)}(F')$. Thus, (5.12) is proven. Finally, (5.13) is trivial. □

Lemma 5.9. *Let $F \in \mathcal{F}_l$ for some $0 \leq l \leq d-2$, and let $G \in \mathcal{F}_{d-1}(F)$. Define $p^* = \max_{R \in \mathcal{R}(G)} p(R)$ (componentwise). Then,*

$$\left(\frac{\mathsf{H}}{\mathsf{p}^2}\right)^{d-l-1} \|v\|_{0,F}^2 \lesssim \|v\|_{0,G}^2 \qquad \forall v \in \mathbb{Q}_{p^*}(G) .$$

Proof. Using several times (5.3) and (5.5), as well as (2.11), we have

$$\begin{aligned} \|v\|_{0,G}^2 &\simeq \sum_{\xi \in \mathcal{G}_{p^*}(G)} |v(\xi)|^2 w_\xi^G \geq \sum_{\xi \in \mathcal{G}_{p^*}(G) \cap F} |v(\xi)|^2 w_\xi^G \\ &\simeq \left(\frac{\mathsf{H}}{\mathsf{p}^2}\right)^{d-l-1} \sum_{\xi \in \mathcal{G}_{p^*}(F)} |v(\xi)|^2 w_\xi^F \simeq \left(\frac{\mathsf{H}}{\mathsf{p}^2}\right)^{d-l-1} \|v\|_{0,F}^2 . \end{aligned}$$

□

We are now ready to prove condition (3.11).

Proposition 5.10. *For b_δ given in Definition 5.1 and for $\tilde{Q}_\delta$ given in Definition 5.3, one has*

$$b_\delta(v - \tilde{Q}_\delta v, v - \tilde{Q}_\delta v) \lesssim a_\delta(v,v) \qquad \forall v \in V_\delta .$$

Proof. First, we observe that the cardinality of any set $\mathcal{F}_m(F)$ defined in (5.1) is bounded by a quantity depending only on the dimension d. We start from the bound given by Lemma 5.7, and focus on any face $F \in \mathcal{F}_{d-1}$. Using inequality (5.12) of Lemma 5.8 with $l = d-1$, we get

$$\sum_{R \in \mathcal{R}(F)} \|v_R - \tilde{q}_{d-1}\|_{0,F}^2 \lesssim \| [v] \|_{0,F}^2 + \frac{\mathsf{H}}{\mathsf{p}^2} \sum_{F' \in \mathcal{F}_{d-2}(F)} \|v_{R^\sharp(F)} - \tilde{q}_{d-2}\|_{0,F'}^2 .$$

A further application of Lemma 5.8 to each summand on the right hand side of the above inequality, now with $l = d-2$, yields

$$\sum_{R\in\mathcal{R}(F)} \|v_R - \tilde{q}_{d-1}\|_{0,F}^2 \lesssim \|[v]\|_{0,F}^2 + \frac{\mathsf{H}}{\mathsf{p}^2} \sum_{F'\in\mathcal{F}_{d-2}(F)} \sum_{G\in\mathcal{F}_{d-1}(F)} \|[v]_G\|_{0,F'}^2 + \left(\frac{\mathsf{H}}{\mathsf{p}^2}\right)^2 \sum_{F'\in\mathcal{F}_{d-2}(F)} \sum_{F''\in\mathcal{F}_{d-3}(F')} \|v_{R^\sharp(F')} - \tilde{q}_{d-3}\|_{0,F''}^2 .$$

Lemma 5.9 with $l = d-2$ yields $\frac{\mathsf{H}}{\mathsf{p}^2}\|[v]_G\|_{0,F'}^2 \lesssim \|[v]\|_{0,G}^2$. At this point, let us introduce the set $\mathcal{F}_{d-1}^{\cap}(F) = \{G\in\mathcal{F}_{d-1} : G\cap F \neq \emptyset\}$ of all faces intersecting the face F, and let us observe that

$$\frac{\mathsf{H}}{\mathsf{p}^2} \sum_{F'\in\mathcal{F}_{d-2}(F)} \sum_{G\in\mathcal{F}_{d-1}(F)} \|[v]_G\|_{0,F'}^2 \lesssim \sum_{G\in\mathcal{F}_{d-1}^{\cap}(F)} \|[v]\|_{0,G}^2 .$$

On the other hand, we have

$$\sum_{F'\in\mathcal{F}_{d-2}(F)} \sum_{F''\in\mathcal{F}_{d-3}(F')} \|v_{R^\sharp(F')} - \tilde{q}_{d-3}\|_{0,F''}^2 \lesssim \sum_{F''\in\mathcal{F}_{d-3}(F)} \sum_{R\in\mathcal{R}(F'')} \|v_R - \tilde{q}_{d-3}\|_{0,F''}^2 .$$

Thus,

$$\sum_{R\in\mathcal{R}(F)} \|v_R - \tilde{q}_{d-1}\|_{0,F}^2 \lesssim \sum_{G\in\mathcal{F}_{d-1}^{\cap}(F)} \|[v]\|_{0,G}^2 + \left(\frac{\mathsf{H}}{\mathsf{p}^2}\right)^2 \sum_{F''\in\mathcal{F}_{d-3}(F)} \sum_{R\in\mathcal{R}(F'')} \|v_R - \tilde{q}_{d-3}\|_{0,F''}^2 .$$

We now proceed recursively, using Lemmas 5.8 and 5.9 with $l = d-3, d-4, \ldots$. At the j-th stage of recursion, we obtain

$$\sum_{R\in\mathcal{R}(F)} \|v_R - \tilde{q}_{d-1}\|_{0,F}^2 \lesssim \sum_{G\in\mathcal{F}_{d-1}^{\cap}(F)} \|[v]\|_{0,G}^2 + \left(\frac{\mathsf{H}}{\mathsf{p}^2}\right)^{j-1} \sum_{F'\in\mathcal{F}_{d-j}(F)} \sum_{R\in\mathcal{R}(F')} \|v_R - \tilde{q}_{d-j}\|_{0,F'}^2 .$$

When $j = d$, we use (5.13) and (5.5) to finally get

$$\sum_{R\in\mathcal{R}(F)} \|v_R - \tilde{q}_{d-1}\|_{0,F}^2 \lesssim \sum_{G\in\mathcal{F}_{d-1}^{\cap}(F)} \|[v]\|_{0,G}^2 .$$

At last, we observe that $\omega_G \simeq \omega_F$ for all $G\in\mathcal{F}_{d-1}^{\cap}(F)$ by (5.6), so that, going back to Lemma 5.7, we conclude that

$$b_\delta(v - \tilde{Q}_\delta v, v - \tilde{Q}_\delta v) \lesssim \sum_{G\in\mathcal{F}_{d-1}} \omega_G \|[v]\|_{0,G}^2 \le a_\delta(v,v) .$$

□

5.4 Summary of Stage I

Thus, all requirements of the Auxiliary Space Method are satisfied for the quantities defined in Sect. 5.2. Note that the Gramian $\mathbf{B}$ of the form b_δ is diagonal so that $\mathbf{C}_\mathbf{B} = \mathbf{B}^{-1}$ is efficiently applicable and trivially satisfies the respective requirements in Corollary 3.4. The quantitative performance of this preconditioning stage will be discussed in Sect. 8. So it remains to construct a suitable preconditioner $\mathbf{C}_{\tilde{\mathbf{A}}}$ for the "auxiliary space problem" involving the bilinear form $\tilde{a}$. Several possible routes to proceed from here suggest themselves. The first one is employ a domain decomposition strategy in the spirit of [25]. This is carried out in [16] where a dual-primal preconditioner for the auxiliary problem is formulated and analyzed. Specifically, the resulting condition numbers are shown to exhibit only a mild square logarithmic growth with respect to polynomial degrees similar to those obtained in [25] for constant degrees.

Here we pursue a different route trying to develop a preconditioner $\mathbf{C}_{\tilde{\mathbf{A}}}$ that eventually gives rise to uniformly bounded condition numbers for the auxiliary problem and hence also for the original problem. Recall that the main obstruction to employing the low order LGL-grid finite elements as a next-stage auxiliary space for the conforming high order space is the non-matching of the LGL grids of different degrees at element interfaces which, in turn, is closely related to the fact that the LGL-grids are not nested. A key element of our approach is to construct certain low order auxiliary spaces that are in some sense "stable companions" of the low order LGL finite elements but that are nested. However, having overcome the principal hurdle of non-nestedness certain further difficulties arise that will be addressed throughout the remainder of this paper.

6 Piecewise polynomial spaces over LGL and dyadic meshes

This section contains preparatory material for the realization of the subsequent stage **SE-CG** $\rightarrow$ **DFE-CG**, see Sect. 4. After recalling some further properties of the LGL-grids introduced in Sect. 2, we turn to the following crucial task. We develop an algorithm to associate to any LGL-grid a *dyadic* grid in such a way that nestedness is guaranteed as the polynomial degree increases. Several approximation operators related to these grids are defined, and certain stability properties are established. Finally, the previous univariate results are extended by tensorization to the multivariate setting which eventually allow us to use these dyadic grids in place of LGL-grids for the construction of low order auxiliary spaces.

Let us introduce a few notations which will be used throughout the section. Given a bounded interval $I = [a, b] \subset R$, consider an ordered grid $\mathcal{G} = \{\xi_j : 0 \leq j \leq p\} \subset I$, with

$$a = \xi_0 < \cdots < \xi_{j-1} < \xi_j < \cdots < \xi_p = b \, .$$

The collection of intervals $I_j = [\xi_{j-1}, \xi_j]$, $1 \leq j \leq p$, defines a finite partition (or mesh) of I, which will be indicated by $\mathcal{T} = \mathcal{T}(\mathcal{G})$. Conversely, any finite partition $\mathcal{T}$ of I comes from a unique ordered grid $\mathcal{G} = \mathcal{G}(\mathcal{T})$; for this reason, the two concepts will be often used equivalently in the sequel. We denote by $h_j = \xi_j - \xi_{j-1} = |I_j|$ the length of the interval $I_j \in \mathcal{T}$. Furthermore, we associate to the partition $\mathcal{T}$ the space of continuous, piecewise-linear functions

$$V_h(\mathcal{T}) = \{v \in C^0(I) \, : \, v_{|I_j} \in \mathbb{P}_1 \, , \; \forall I_j \in \mathcal{T}\} \, . \tag{6.1}$$

The following definitions will be crucial in the sequel.

Definition 6.1. *An ordered grid $\mathcal{G} = \{\xi_j : 0 \leq j \leq p\}$ in I is locally C_g-quasiuniform if there exists a constant $C_g > 1$ such that*

$$C_g^{-1} \leq \frac{|I_{j+1}|}{|I_j|} \leq C_g \, , \qquad 1 \leq j \leq p-1 \, . \tag{6.2}$$

Definition 6.2. *An ordered grid $\mathcal{G}$ in I is locally (A, B)-uniformly equivalent to another ordered grid $\tilde{\mathcal{G}}$ if there exist constants $0 < A < B$ such that*

$$\forall I_j \in \mathcal{T}(\mathcal{G}), \quad \forall \tilde{I}_l \in \mathcal{T}(\tilde{\mathcal{G}}) \, , \qquad I_j \cap \tilde{I}_l \neq \emptyset \implies A \leq \frac{|I_j|}{|\tilde{I}_l|} \leq B \, . \tag{6.3}$$

Examples are given by the LGL-grids and the associated dyadic grids, as discussed below.

6.1 LGL-grids and finite elements

Given any integer $p > 0$, let $\mathcal{G}_p(I)$ be the LGL-grid of order p in I and let $\mathcal{T}_p(I) = \mathcal{T}(\mathcal{G}_p(I))$ be the corresponding partition. We recall that the points in $\mathcal{G}_p(I)$ are symmetrically placed around the center of the interval, and the intervals in $\mathcal{T}_p(I)$ are monotone in the sense that

$$I_j,\, I_{j+1} \in \mathcal{T}_p(I), \quad I_j,\, I_{j+1} \subset [a, (a+b)/2] \quad \Rightarrow \quad |I_j| < |I_{j+1}| \,, \tag{6.4}$$

with the analogous reverse relation for the right half $[(a+b)/2, b]$ of I. Furthermore, the variation of the interval lengths is uniformly smooth, in the sense that $\mathcal{G}_p(I)$ is locally C_g-quasiuniform for a constant $C_g > 1$ *independent of* p. These results can be found, e.g., in [8].

Another relevant property concerns the locally uniform equivalence of LGL-grids of comparable order; we refer to [8] for the proof.

Property 6.3. *Assume that $cp \le q \le p$ for some fixed constant $c > 0$. Then, $\mathcal{G}_q(I)$ and $\mathcal{G}_p(I)$ are locally (A, B)-uniformly equivalent, with A and B depending on the proportionality factor c but independent of q and p.*

A crucial role in what follows will be played by the relation between the high-order polynomial space $V_p(I) := \mathbb{P}_p(I)$ and its low-order *companion finite element space* $V_{h,p}(I) = V_h(\mathcal{T}_p(I))$ of the continuous, piecewise-linear functions on the partition $\mathcal{T}_p(I)$. Let us introduce the interpolation operators at the nodes of $\mathcal{G}_p(I)$

$$\begin{aligned} &\mathcal{I}_p : C^0(I) \to \mathbb{P}_p(I) \,, && \mathcal{I}_{h,p} : C^0(I) \to V_{h,p}(I) \,, && \\ &(\mathcal{I}_p v)(\xi_j) = v(\xi_j) \,, && (\mathcal{I}_{h,p} v)(\xi_j) = v(\xi_j) \,, && 0 \le j \le p \,, \quad \forall v \in C^0(I) \,. \end{aligned} \tag{6.5}$$

Then, $v \mapsto v_h = \mathcal{I}_{h,p} v$ defines an isomorphism between $\mathbb{P}_p(I)$ and $V_{h,p}(I)$, with inverse $v_h \mapsto v = \mathcal{I}_p v_h$. The next property provides uniform equivalences between norms of global polynomials and their piecewise affine interpolants at the LGL-grid, and vice-versa, which are at the core of the subsequent applications to preconditioning (see [13, 23]).

Property 6.4. *One has*

$$\|v\|_{0,I} \simeq \|v_h\|_{0,I} \qquad \forall v \in \mathbb{P}_p(I) \,, \tag{6.6}$$

and

$$\|v'\|_{0,I} \simeq \|v_h'\|_{0,I} \qquad \forall v \in \mathbb{P}_p(I) \,, \tag{6.7}$$

where the involved constants are independent of p and $H = b - a$.

Note that taking as v in (6.6) each Lagrange basis function at the LGL nodes and using (2.2) and (6.2), it is easily seen that the size of each interval I_j is comparable to that of the LGL weight associated with any of its endpoints, in the sense that the following bounds hold, uniformly in p and H:

$$1 \lesssim \min_{1 \le j \le p} \frac{h_j}{w_j} \;\le\; \max_{1 \le j \le p} \frac{h_j}{w_j} \lesssim 1 \,. \tag{6.8}$$

As a consequence, (6.7) together with (6.8) and (2.2) provide a simple proof of the inverse inequality (2.6). Indeed, one has

$$\|v_h'\|_{0,I} = \sum_{j=1}^{p} \left(\frac{v(\xi_j) - v(\xi_{j-1})}{h_j} \right)^2 h_j \le \frac{2}{h_0} v^2(\xi_0) + \sum_{j=1}^{p-1} \left(\frac{2}{h_j} + \frac{2}{h_{j+1}} \right) v^2(\xi_j) + \frac{2}{h_p} v^2(\xi_p) \,.$$

6.2 Dyadic meshes

The subsequent stage **SE-CG** $\rightarrow$ **DFE-CG** will rely upon the use of auxiliary spaces based on dyadic grids that are in a certain sense associated with LGL-grids, but have the additional advantage of giving rise to *nested conforming* spaces. Their construction, based on recursion algorithms, is detailed in [8] (see also [9] for an extensive quantitative investigation of their properties). Hereafter, we summarize the main results that are needed in the subsequent analysis, referring to [8] and [9] for their proofs.

We wish to construct for a given ordered grid $\mathcal{G}$ in I an "equivalent" (in the sense of the definition above) dyadic mesh $\mathcal{D}$. To this end, it will be convenient to introduce for any interval D

$$\overline{I}(D,\mathcal{G}) := \operatorname{argmax}\left\{|I_j| : I_j \in \mathcal{T}(\mathcal{G}),\ D \cap I_j \neq \emptyset\right\} . \tag{6.9}$$

Given a real $\alpha > 0$ and an initial dyadic partition $\mathcal{D}_0$, a dyadic partition $\mathcal{D}$ can be constructed recursively as follows:

Dyadic $[\mathcal{G}, \mathcal{D}_0, \alpha] \rightarrow \mathcal{D}$:

(i) Set $\mathcal{D} := \mathcal{D}_0$.

(ii) While there exists $D \in \mathcal{D}$ *such that*

$$|D| > \alpha|\overline{I}(D,\mathcal{G})| \tag{6.10}$$

split D *by halving it and replace it by its two children* D', D'', $D = D' \cup D''$, *i.e.*

$$(\mathcal{D} \setminus \{D\}) \cup \{D', D''\} \rightarrow \mathcal{D}.$$

Such a dyadic mesh generator, applied to the sequence of LGL-grids $\mathcal{G}_p = \mathcal{G}_p(I)$, produces meshes $\mathcal{D}_p^* :=$ **Dyadic** $[\mathcal{G}_p, \{I\}, \alpha]$ which enjoy additional structural properties useful for our purposes. First, as the sets $\mathcal{G}_p$ are symmetric around the center of the interval, so will be the grids $\mathcal{D}_p^*$, always containing the center as a node. Next, a major requirement on the dyadic partitions associated with the $\mathcal{G}_p$'s is that they are nested, which will later be essential in the context of the ASM. Unfortunately, numerical evidence shows that the grids $\mathcal{D}_p^*$ are not necessarily nested, although exceptions seem to be very rare (see [9]). Thus, in order to ensure nestedness of the generated dyadic meshes, we shall employ the following recursive definition:

$\mathcal{G}_p \rightarrow \mathcal{D}_p$:

(i) Given $\alpha > 0$, *set*

$$\mathcal{D}_1 := \textbf{Dyadic}[\mathcal{G}_1, \{I\}, \alpha].$$

(ii) For $p > 1$, *given* $\mathcal{D}_{p-1}$, *set*

$$\mathcal{D}_p := \textbf{Dyadic}[\mathcal{G}_p, \mathcal{D}_{p-1}, \alpha]. \tag{6.11}$$

Property 6.5. *For all* $p \geq 1$, *the dyadic meshes* $\mathcal{D}_p$ *are nested and locally* (A,B)*-uniformly equivalent to* $\mathcal{G}_p$ *with constants* A, B *specified as follows:*

$$\forall D \in \mathcal{D}_p\ , \quad \forall I_j \in \mathcal{T}_p\ , \qquad I_j \cap D \neq \emptyset \quad \Longrightarrow \quad A := \alpha^{-1} \leq \frac{|I_j|}{|D|} \leq \frac{2C_g}{\min\{\alpha C_g^{-1}, 1\}} =: B\ . \tag{6.12}$$

Furthermore,

$$\operatorname{card} \mathcal{D}_p \simeq \operatorname{card} \mathcal{G}_p\ . \tag{6.13}$$

In order to keep the cardinality of $\mathcal{D}_p$ as close as possible to that of $\mathcal{G}_p$, numerical evidence suggests to choose the parameter $\alpha \geq 1$, to guarantee gradedness of the dyadic mesh, but close to 1, to avoid excessively many points in the dyadic mesh, see [9] for more details.

The following useful generalization is an easy consequence of Properties 6.3 and 6.5.

Corollary 6.6. *Assume that $c\,p \leq q \leq p$ for some fixed constant $c > 0$. Then, $\mathcal{D}_q$ is locally (A, B)-uniformly equivalent to both $\mathcal{G}_p$ and $\mathcal{D}_p$, with A and B depending on the proportionality factor c but not on p.*

6.3 Stability results for univariate interpolation operators

In the rest of the paper, we assume that we have fixed a value $\alpha \geq 1$ close to 1 and consequently for any interval I we have generated by the recursion (6.11) the sequence $\mathcal{D}_p(I)$ of dyadic meshes associated with the LGL-grids $\mathcal{G}_p(I)$. Let $\mathcal{G}_{D,p}(I)$ denote the set of dyadic nodes in I which define the partition $\mathcal{D}_p(I)$, i.e., such that $\mathcal{D}_p(I) = \mathcal{T}(\mathcal{G}_{D,p}(I))$. Furthermore, let us introduce the finite element space

$$V_{h,D,p}(I) = V_h(\mathcal{D}_p(I)) = \{v \in C^0(I) \,:\, v_{|D} \in \mathbb{P}_1 \,,\ \forall D \in \mathcal{D}_p(I)\} \tag{6.14}$$

of the continuous, piecewise linear functions on the partition $\mathcal{D}_p(I)$, and let

$$\mathcal{I}_{h,D,p} : C^0(I) \to V_{h,D,p}(I) \,, \qquad (\mathcal{I}_{h,D,p}v)(\zeta) = v(\zeta) \quad \forall \zeta \in \mathcal{G}_{D,p}(I) \,,\ \ \forall v \in C^0(I) \,, \tag{6.15}$$

be the interpolation operator at the nodes of $\mathcal{G}_{D,p}(I)$. We also introduce the composite interpolation operator

$$\mathcal{K}_{h,D,p} : C^0(I) \to V_{h,D,p}(I) \,, \qquad \mathcal{K}_{h,D,p} = \mathcal{I}_{h,D,p} \circ \mathcal{I}_{h,p} \,. \tag{6.16}$$

We proceed now to establish various stability results involving these operators.

Lemma 6.7. *Let $\mathcal{G}$ be any ordered grid in I, which defines a partition $\mathcal{T} = \mathcal{T}(\mathcal{G})$, and let $\mathcal{I}_{\mathcal{G}} : H^1(I) \to V_h(\mathcal{T})$ be the associated piecewise linear interpolation operator. Then,*

$$|\mathcal{I}_{\mathcal{G}}v|_{1,I} \leq |v|_{1,I} \qquad \forall v \in H^1(I) \,.$$

Proof. Let $\mathcal{G} = \{\xi_j \,:\, 0 \leq j \leq p\}$, with $h_j = \xi_j - \xi_{j-1}$. Then,

$$|\mathcal{I}_{\mathcal{G}}v|^2_{1,I} = \sum_{j=1}^{p} \int_{\xi_{j-1}}^{\xi_j} \left(\frac{v(\xi_j) - v(\xi_{j-1})}{h_j} \right)^2 dx = \sum_{j=1}^{p} \frac{1}{h_j} \left(v(\xi_j) - v(\xi_{j-1}) \right)^2 \,.$$

Writing $v(\xi_j) - v(\xi_{j-1}) = \int_{\xi_{j-1}}^{\xi_j} \frac{dv}{dx}$ and using the Cauchy-Schwarz inequality, we obtain

$$\left(v(\xi_j) - v(\xi_{j-1}) \right)^2 \leq h_j \int_{\xi_{j-1}}^{\xi_j} \left(\frac{dv}{dx} \right)^2 ,$$

whence the result follows. □

Lemma 6.8. *Let $\mathcal{G}$ and $\tilde{\mathcal{G}}$ be ordered grids in I, with associated partitions $\mathcal{T} = \mathcal{T}(\mathcal{G})$ and $\tilde{\mathcal{T}} = \mathcal{T}(\tilde{\mathcal{G}})$. Assume that $\mathcal{G}$ and $\tilde{\mathcal{G}}$ are locally (A, B)-uniformly equivalent. If $\mathcal{I}_{\mathcal{G}} : H^1(I) \to V_h(\mathcal{T})$ is the piecewise linear interpolation operator associated with $\mathcal{G}$, one has*

$$\|\mathcal{I}_{\mathcal{G}}v\|_{0,I} \lesssim \|v\|_{0,I} \qquad \forall v \in V_h(\tilde{\mathcal{T}}) \,,$$

where the constant in the inequality depends only on the parameters A and B.

Proof. Let $\mathcal{G} = \{\xi_j : 0 \le j \le p\}$ and $\mathcal{T} = \{I_j : 1 \le j \le p\}$, with $h_j = |I_j| = \xi_j - \xi_{j-1}$. Let us set

$$h(\xi_j) = \begin{cases} h_1 & \text{if } j = 0 \ , \\ h_j + h_{j+1} & \text{if } 1 \le j \le p-1 \ , \\ h_p & \text{if } j = p \ . \end{cases} \tag{6.17}$$

Similarly, let $\tilde{\mathcal{G}} = \{\eta_i : 0 \le i \le q\}$ and $\tilde{\mathcal{T}} = \{\tilde{I}_i : 1 \le i \le q\}$, with $\tilde{h}_i = |\tilde{I}_i| = \eta_i - \eta_{i-1}$. Furthermore, let $\tilde{h}(\eta_i)$ be defined in a manner similar to (6.17). Given any $v \in V_h(\tilde{\mathcal{T}})$, we have

$$\|\mathcal{I}_{\mathcal{G}} v\|_{0,I}^2 = \sum_{j=1}^{p} \|\mathcal{I}_h v\|_{0,I_j}^2 \simeq \sum_{j=1}^{p} \left(v^2(\xi_j) + v^2(\xi_{j-1})\right) h_j = \sum_{j=0}^{p} v^2(\xi_j) h(\xi_j) \ ,$$

and

$$\|v\|_{0,I}^2 = \sum_{i=1}^{q} \|v\|_{0,\tilde{I}_i}^2 \simeq \sum_{i=1}^{q} \left(v^2(\eta_i) + v^2(\eta_{i-1})\right) \tilde{h}_i = \sum_{i=0}^{q} v^2(\eta_i) \tilde{h}(\eta_i) \ .$$

Now, for any ξ_j there exist η_i and $\theta \in [0,1)$ such that $v(\xi_j) = (1-\theta) v(\eta_i) + \theta v(\eta_{i+1})$, whence $v^2(\xi_j) \le v^2(\eta_i) + v^2(\eta_{i+1})$. If $\theta \in (0,1)$, then $\xi_j \in (\eta_i, \eta_{i+1})$, hence both I_j and I_{j+1} intersect $\tilde{I}_i$. By the assumption of locally uniform equivalence of the two grids, we obtain $|I_j| \lesssim |\tilde{I}_i|$ and $|I_{j+1}| \lesssim |\tilde{I}_i|$, whence $h(\xi_j) \lesssim \tilde{h}_i \le \min\left(\tilde{h}(\eta_i), \tilde{h}(\eta_{i+1})\right)$. On the other hand, if $\theta = 0$, i.e., $\xi_j = \eta_i$, then I_j intersects $\tilde{I}_i$ and I_{j+1} intersects $\tilde{I}_{i+1}$ (with the obvious adaptation if ξ_j is a boundary point), thus $|I_j| \lesssim |\tilde{I}_i|$ and $|I_{j+1}| \lesssim |\tilde{I}_i|$, which yields $h(\xi_j) \lesssim \tilde{h}(\eta_i)$. This completes the proof. ☐

From now on, let $\mathcal{I}_p$, $\mathcal{I}_{h,p}$, $\mathcal{I}_{h,D,p}$, and $\mathcal{K}_{h,D,p}$, resp., be the interpolation operators defined in (6.5), (6.15) and (6.16), resp..

Property 6.9. *For any $p > 0$, the operator $\mathcal{I}_p$ satisfies*

$$|\mathcal{I}_p v|_{1,I} \lesssim |v|_{1,I} \ , \qquad \forall v \in H^1(I) \ ,$$

with a constant that does not depend on p.

Proof. The result is classical (see, e.g., [15]). It can be derived from Property 6.4 and Lemma 6.7 observing that $\mathcal{I}_p v = \mathcal{I}_p(\mathcal{I}_{h,p} v)$. ☐

Property 6.10. [5, Remark 13.5] *Assume that $cp \le q \le p$ for some fixed constant $c > 0$. Then*

$$\|\mathcal{I}_q v\|_{0,I} \lesssim \|v\|_{0,I} \quad \forall v \in \mathbb{P}_p(I) \ ,$$

with a constant depending on the proportionality factor c but not on p.

Property 6.11. *Assume that $cp \le q \le p$ for some fixed constant $c > 0$. Then,*

$$|\mathcal{I}_{h,q} v|_{m,I} \lesssim |v|_{m,I} \quad \forall v \in \mathbb{P}_p(I) \ , \qquad m = 0, 1 \ ,$$

with a constant depending on the proportionality factor c but not on p.

Proof. For $m = 0$, we observe that $\mathcal{I}_{h,q} v = \mathcal{I}_{h,q}(\mathcal{I}_q v)$, so that $\|\mathcal{I}_{h,q} v\|_{0,I} \lesssim \|\mathcal{I}_q v\|_{0,I} \lesssim \|v\|_{0,I}$ by Properties 6.4 and 6.10. The result for $m = 1$ is included in Lemma 6.7. ☐

Property 6.12. *Assume that $cp \le q \le p$ for some fixed constant $c > 0$. Then, for $m = 0, 1$ one has*

$$\begin{aligned} |\mathcal{I}_q v|_{m,I} \ \simeq \ |\mathcal{I}_{h,q} v|_{m,I} &\lesssim |v|_{m,I} \quad \forall v \in V_{h,D,p}(I) \ , \\ |\mathcal{I}_{h,D,q} v|_{m,I} &\lesssim |v|_{m,I} \quad \forall v \in V_{h,D,p}(I) \ , \\ |\mathcal{I}_{h,D,q} v|_{m,I} &\lesssim |v|_{m,I} \quad \forall v \in V_{h,p}(I) \ . \end{aligned}$$

Proof. The results for $m = 0$ follow from Lemma 6.8 applied in various combinations to the grids $\mathcal{G}_q(I)$, $\mathcal{G}_p(I)$, $\mathcal{D}_q(I)$ and $\mathcal{D}_p(I)$, that are locally uniformly equivalent to each other by Corollary 6.6. The results for $m = 1$ follow again from Lemma 6.7. □

Combining the bounds in the two previous properties, we obtain the following result.

Property 6.13. *Assume that $c\,p \leq q \leq p$ for some fixed constant $c > 0$. Then one has*

$$|\mathcal{K}_{h,D,q} v|_{m,I} \lesssim |v|_{m,I} \quad \forall v \in \mathbb{P}_p(I) \;, \qquad m = 0, 1 \;.$$

6.4 Tensor-product interpolation operators

Tensorization of the univariate interpolation operators considered above yields multivariate interpolation operators on (hyper-)rectangles. Given any such element $R = \times_{k=1}^{d} I_k \in \mathcal{R}$ as defined in (2.7), let

$$\mathcal{I}_p = \mathcal{I}_p^R \;:\; C^0(R) \to \mathbb{Q}_p(R) \;, \qquad \mathcal{I}_p^R = \bigotimes_{k=1}^{d} \mathcal{I}_{p_k}^{I_k} \tag{6.18}$$

be the global polynomial interpolation operator at the nodes of the tensor product LGL-grid $\mathcal{G}_p(R)$ introduced in (2.8). On the other hand, let $\mathcal{T}_p(R) = \mathcal{T}(\mathcal{G}_p(R))$ be the partition of R into (hyper-)rectangles $S = S_\ell = \times_{k=1}^{d} I_{k,\ell_k}$ for $\ell \in \times_{k=1}^{d}\{1, \ldots, p_k\}$, where each I_{k,ℓ_k} is an interval in the partition $\mathcal{T}_{p_k}(I_k)$ of I_k. Then, we set

$$V_{h,p}(R) = \{v \in C^0(R) \;:\; v_{|S} \in \mathbb{Q}_1 \;\; \forall S \in \mathcal{T}_p(R)\} = \bigotimes_{k=1}^{d} V_{h,p_k}(I_k) \;, \tag{6.19}$$

and introduce the piecewise multilinear interpolation operator on the LGL-grid $\mathcal{G}_p(R)$

$$\mathcal{I}_{h,p} = \mathcal{I}_{h,p}^R \;:\; C^0(R) \to V_{h,p}(R) \;, \qquad \mathcal{I}_{h,p}^R = \bigotimes_{k=1}^{d} \mathcal{I}_{h,p_k}^{I_k} \;. \tag{6.20}$$

Similarly, let $\mathcal{D}_p(R) = \mathcal{T}(\mathcal{G}_{D,p}(R))$ be the partition of R into dyadic (hyper-)rectangles $E = E_m = \times_{k=1}^{d} D_{k,m_k}$, where each D_{k,m_k} is a dyadic interval in the partition $\mathcal{D}_{p_k}(I_k)$ of I_k. Then, we set

$$V_{h,D,p}(R) = \{v \in C^0(R) \;:\; v_{|E} \in \mathbb{Q}_1 \;\; \forall E \in \mathcal{D}_p(R)\} = \bigotimes_{k=1}^{d} V_{h,D,p_k}(I_k) \;, \tag{6.21}$$

and introduce the piecewise multilinear interpolation operator on the associated dyadic grid $\mathcal{G}_{D,p}(R)$

$$\mathcal{I}_{h,D,p} = \mathcal{I}_{h,D,p}^R \;:\; C^0(R) \to V_{h,D,p}(R) \;, \qquad \mathcal{I}_{h,D,p}^R = \bigotimes_{k=1}^{d} \mathcal{I}_{h,D,p_k}^{I_k} \;. \tag{6.22}$$

Finally, we set

$$\mathcal{K}_{h,D,p} = \mathcal{K}_{h,D,p}^R \;:\; C^0(R) \to V_{h,D,p}(R) \;, \qquad \mathcal{K}_{h,D,p}^R = \mathcal{I}_{h,D,p}^R \circ \mathcal{I}_{h,p}^R \;. \tag{6.23}$$

Given any l-dimensional facet $F \in \mathcal{F}_l$, the analogous definition of the finite dimensional spaces $\mathbb{Q}_p(F)$, $V_{h,p}(F)$ and $V_{h,D,p}(F)$, as well as the corresponding interpolation operators $\mathcal{I}_p^F$, $\mathcal{I}_{h,p}^F$ and $\mathcal{I}_{h,D,p}^F$, is straightforward.

The analysis of our tensor-product interpolation operators relies on the following classical result.

Proposition 6.14. *For $1 \le k \le d$, let W_k, $V_k \subset H^1(I_k)$ be finite dimensional subspaces. Let $L_k : W_k \to V_k$ be linear operators satisfying, for $m = 0, 1$,*

$$\|L_k v\|_{m,I_k} \lesssim \|v\|_{m,I_k} \quad \forall v \in W_k \; . \tag{6.24}$$

Then, setting $W := \bigotimes_{k=1}^d W_k$ and $V := \bigotimes_{k=1}^d V_k$, the operator $A = \bigotimes_{k=1}^d A_k : W \to V$ satisfies, for $m = 0, 1$,

$$\|Lv\|_{m,R} \lesssim \|v\|_{m,R} \quad \forall v \in W \; . \tag{6.25}$$

In addition, if the norms in (6.24) *for $m = 1$ can be replaced by seminorms, i.e.,*

$$|L_k v|_{1,I_k} \lesssim |v|_{1,I_k} \quad \forall v \in W_k, \quad 1 \le k \le d \; , \tag{6.26}$$

then, the same occurs in (6.25) *for $m = 1$, i.e.,*

$$Lv|_{1,R} \lesssim |v|_{1,R} \quad \forall v \in W \; . \tag{6.27}$$

The first consequence of this result is the multidimensional version of Property 6.4. It states that the operator $\mathcal{I}^R_{h,p}$ induces a topological isomorphims between $\mathbb{Q}_p(R)$ and $V_{h,p}(R)$ equipped with the L^2 or H^1 norms, whose inverse is induced by $\mathcal{I}^R_p$.

Property 6.15. *For any $v \in \mathbb{Q}_p(R)$, set $v_h := \mathcal{I}^R_{h,p}(v)$. Then,*

$$\|v\|_{0,R} \simeq \|v_h\|_{0,R} \qquad \text{and} \qquad \|\nabla v\|_{0,R} \simeq \|\nabla v_h\|_{0,R} \; . \tag{6.28}$$

The constants in both relations are independent of p and H.

Using Lemmas 6.7 and 6.8, Proposition 6.14 yields the following general result.

Property 6.16. *For $1 \le k \le d$, let $\mathcal{G}_k$ and $\tilde{\mathcal{G}}_k$ be ordered grids in I_k, with associated partitions $\mathcal{T}_k$ and $\tilde{\mathcal{T}}_k$, which are locally (A, B)-uniformly equivalent; let $\mathcal{I}_{\mathcal{G}_k} = \mathcal{I}^{I_k}_{\mathcal{G}_k} : H^1(I_k) \to V_h(\mathcal{T}_k)$ be the piecewise linear interpolation operator associated with $\mathcal{T}_k$. Consider the spaces $V_h(\mathcal{T}) := \bigotimes_{k=1}^d V_h(\mathcal{T}_k)$ and $V_h(\tilde{\mathcal{T}}) := \bigotimes_{k=1}^d V_h(\tilde{\mathcal{T}}_k)$ of piecewise multi-linear functions on the cartesian partitions $\mathcal{T} := \bigtimes_{k=1}^d \mathcal{T}_k$ and $\tilde{\mathcal{T}} := \bigtimes_{k=1}^d \tilde{\mathcal{T}}_k$ of R. Then, the piecewise multilinear interpolation operator $\mathcal{I}_{\mathcal{G}} = \mathcal{I}^R_{\mathcal{G}} := \bigotimes_{k=1}^d \mathcal{I}^{I_k}_{\mathcal{G}_k} : C^0(R) \to V_h(\mathcal{T})$ satisfies*

$$\|\mathcal{I}_{\mathcal{G}} v\|_{m,R} \lesssim \|v\|_{m,R} \qquad \forall v \in V_h(\tilde{\mathcal{T}}) \; , \qquad m = 0, 1 \; ,$$

where the constant in the inequality depends only on the parameters A and B.

In the sequel, the inequality $q \le p$ between two multi-indices $p, q \in \mathbb{N}^d$ is to be understood componentwise, i.e., $q_k \le p_k$ for all k. From Property 6.12 and Proposition 6.14, we immediately get the following multidimensional result.

Property 6.17. *Assume that $c\,p \le q \le p$ for some fixed constant $c > 0$. Then,*

$$|\mathcal{I}_q v|_{m,R} \lesssim |v|_{m,R} \quad \forall v \in V_{h,D,p}(R) \; , \qquad m = 0, 1 \; ,$$

with a constant depending on the proportionality factor c but not on p.

Finally, from Property 6.13 and Proposition 6.14, we immediately get the following multivariate result.

Property 6.18. *Assume that $c\,p \le q \le p$ for some fixed constant $c > 0$. Then,*

$$|\mathcal{K}_{h,D,p} v|_{m,R} \lesssim |v|_{m,R} \quad \forall v \in \mathbb{Q}_p(R) \; , \qquad m = 0, 1 \; ,$$

with a constant depending on the proportionality factor c but not on p.

6.5 A localized Jackson estimate for the interpolation error

For the verification of certain ASM conditions in the next section, we will need Jackson estimates for piecewise multilinear interpolation errors, which involve the meshsize in a localized, cell-wise manner. Since these results will be applied to both the LGL- and the dyadic tensorized grids, with various choices of finite-dimensional function spaces (comprised of either piecewise multi-linear or global polynomial functions), we first establish the key estimates in suitable generality in order to specialize them later to the cases at hand.

Consider again the general piecewise multilinear interpolation operator $\mathcal{I}_\mathcal{G} = \mathcal{I}_\mathcal{G}^R : C^0(R) \to V_h(\mathcal{T})$ introduced in the statement of Property 6.16 above. In addition, assume that each grid $\mathcal{G}_k$ is locally quasiuniform according to Definition 6.1. For $k = 1, \dots, d$, let W_k be a finite dimensional subspace of $H^1(I_k)$ to be specified later. Then, the univariate piecewise linear interpolation operator $\mathcal{I}_{\mathcal{G}_k} = \mathcal{I}_{\mathcal{G}_k}^{I_k}$ is well-defined on W_k and we have

$$\|\mathcal{I}_{\mathcal{G}_k} v\|_{0,I_k} \le \bar{c}_k \|v\|_{0,I_k} \qquad \forall v \in W_k \ , \tag{6.29}$$

for some constant $\bar{c}_k > 0$ independent of the size $|I_k|$ but possibly depending on the dimension of W_k (although this will not be the case in all our applications). Let us set $W = \bigotimes_{k=1}^d W_k$.

Next, consider the cells S_ℓ forming the partition $\mathcal{T} = \times_{k=1}^d \mathcal{T}_k$, i.e., $\mathcal{T} = \{S_\ell = \times_{k=1}^d I_{k,\ell_k} \ : I_{k,\ell_k} \in \mathcal{T}_k\}$, and let $h_\ell := \max_k |I_{k,\ell_k}|$ be the largest one-dimensional size of the cell S_ℓ. Let $h = \sum_\ell h_\ell \chi_{S_\ell}$ be the meshsize function defined in R.

The following *localized* Jackson estimate will be used several times in Sect. 7 for proving certain ASM conditions.

Proposition 6.19. *The following estimate holds*

$$\|h^{-1}(v - \mathcal{I}_\mathcal{G} v)\|_{0,R} \lesssim |v|_{1,R} \qquad \forall v \in W \ , \tag{6.30}$$

where the constant implied by the inequality is independent of the meshsize but depends on the constants $\bar{c}_k$ introduced in (6.29).

Proof. The result will be obtained by assembling local estimates in each cell S_ℓ, which in turn are derived by a scaling argument from corresponding estimates on the unit box $B^d = [0,1]^d$, with $B = [0,1]$. To this end, let $\mathcal{I}_{B^k} := \mathcal{I}_1^{B^k}$ denote the multilinear interpolation operator on B^k, i.e.,

$$\mathcal{I}_{B^k} v = \sum_{\xi \in \mathcal{F}_0(B^k)} v(\xi) \Phi_\xi \ ,$$

where Φ_ξ denotes the multilinear Lagrange basis function satisfying $\Phi_\xi(\xi') = \delta_{\xi,\xi'}$ for $\xi, \xi' \in \mathcal{F}_0(B^k)$. We make heavy use of the fact that $\mathcal{I}_{B^d}$ is a tensor product operator, i.e., we have $\mathcal{I}_{B^d} = \otimes^d \mathcal{I}_B$. Moreover, it will be convenient to employ the following convention to write, for any $k = 1, \dots, d$,

$$B^d = A^k \times B^{d-k} \ ,$$

meaning that A^k is the unit k-cube representing the first k variables and B^{d-k} is the unit $(d-k)$-cube for the coordinates $d-k+1, \dots, d$, .

Lemma 6.20. *Let $\mathcal{W} = \bigotimes_{k=1}^d \mathcal{W}_k$, where $\mathcal{W}_k$ are finite-dimensional subspaces of $H^1(B)$. Then, one has*

$$\|v - \mathcal{I}_{B^d} v\|_{0,B^d}^2 \lesssim \sum_{k=1}^d \sum_{\xi \in \mathcal{G}(A^{k-1})} \|\partial_{x_k} v(\xi, \cdot)\|_{0,B^{d-k+1}}^2 \ , \qquad \forall v \in \mathcal{W} \ , \tag{6.31}$$

(with the first summand on the right-hand side to be understood as $\|\partial_{x_1} v\|_{0,B^d}^2$), where the constant depends only on d.

Proof. Notice first that for $e := v - \mathcal{I}_B v$ one has $(\mathcal{I}_B v)' = v(1) - v(0) = \int_0^1 v'(s)ds$ so that $e(x) = \int_0^x v'(s)ds - x\int_0^1 v'(s)ds$ from which one easily derives that

$$\|v - \mathcal{I}_B v\|_{0,B} \le 2|v|_{1,B}, \quad v \in H^1(B). \tag{6.32}$$

Next, denoting by id the identity operator on B, and writing

$$\begin{aligned} v - \mathcal{I}_{B^d} v &= \sum_{k=1}^{d} \Big((\mathcal{I}_{B^{k-1}} \otimes \mathrm{id}^{d-k+1})v - (\mathcal{I}_{B^k} \otimes \mathrm{id}^{d-k})v \Big) \\ &= \sum_{k=1}^{d} \big(\mathrm{id}^{k-1} \otimes (\mathrm{id} - \mathcal{I}_B) \otimes \mathrm{id}^{d-k}\big)(\mathcal{I}_{B^{k-1}} \otimes \mathrm{id}^{d-k+1})v, \end{aligned}$$

we note that, when abbreviating $w_k := (\mathcal{I}_{B^{k-1}} \otimes \mathrm{id}^{d-k+1} v)$, for $x_k' := (x_1, , \ldots, x_{k-1}, x_{k+1}, \ldots, x_d)$ one has

$$(\mathrm{id}^{k-1} \otimes (\mathrm{id} - \mathcal{I}_B) \otimes \mathrm{id}^{d-k}) w_k(x_1, \ldots, x_{k-1}, \xi_k, x_{k+1}, \ldots, x_d) = 0, \quad \xi_k = 0, 1, \quad x_k' \in A^{k-1} \times B^{d-k}.$$

Hence, we can apply (6.32) to conclude that

$$\big\| \big(\mathrm{id}^{k-1} \otimes (\mathrm{id} - \mathcal{I}_B) \otimes \mathrm{id}^{d-k}\big) w_k \big\|_{0,B^d} \le 2\|\partial_{x_k} w_k\|_{0,B^d}.$$

For $k \ge 2$, notice that $w_k(\xi, \cdot) = v(\xi, \cdot)$, $\xi \in \mathcal{F}_0(A^{k-1})$ and that w_k is affine in the first $k-1$ variables. Hence, we conclude that

$$\|\partial_{x_k} w_k\|_{0,B^d}^2 \lesssim \sum_{\xi \in \mathcal{F}_0(A^{k-1})} \|\partial_{x_k} v(\xi, \cdot)\|_{0,B^{d-k+1}}^2,$$

from which the assertion of Lemma 6.20 easily follows. □

To complete the proof of Proposition 6.19 consider now a generic cell $S_\ell \in \mathcal{T}$, which we can write as

$$S_\ell = \big(\bigtimes_{l=1}^{k} I_{l,\ell_l} \big) \times \big(\bigtimes_{l=k+1}^{d} I_{l,\ell_l} \big) =: A_\ell^k \times B_\ell^{d-k}.$$

Given any $v \in \mathcal{W}$ and considering its restriction to S_ℓ, we write $\hat{v}(\hat{x}) = v(x)$ with $\hat{x} \in B^d$, so that $(\mathcal{I}_{S_\ell} v)(x) = (\mathcal{I}_{B^d} \hat{v})(\hat{x})$; setting $h_{l,\ell_l} := |I_{l,\ell_l}|$, a standard affine change of variables yields in view of (6.31),

$$\begin{aligned} \|v - \mathcal{I}_{S_\ell} v\|_{0,S_\ell}^2 = |S_\ell| \|\hat{v} - \mathcal{I}_{B^d} \hat{v}\|_{0,B^d}^2 &\lesssim |S_\ell| \sum_{k=1}^{d} \sum_{\xi \in \mathcal{F}_0(A^{k-1})} \|\partial_{\hat{x}_k} \hat{v}(\xi, \cdot)\|_{0,B^{d-k+1}}^2 \\ &\lesssim |S_\ell| \sum_{k=1}^{d} \sum_{\xi \in \mathcal{F}_0(A_\ell^{k-1})} |B_\ell^{d-k+1}|^{-1} h_{k,\ell_k}^2 \|\partial_{x_k} v(\xi, \cdot)\|_{0,B_\ell^{d-k+1}}^2 \\ &\lesssim h_\ell^2 \sum_{k=1}^{d} \sum_{\xi \in \mathcal{F}_0(A_\ell^{k-1})} |A_\ell^{k-1}| \, \|\partial_{x_k} v(\xi, \cdot)\|_{0,B_\ell^{d-k+1}}^2 . \end{aligned} \tag{6.33}$$

Dividing both sides by h_ℓ^2 and summing over ℓ provides

$$\|h^{-1}(v - \mathcal{I}_{\mathcal{G}} v)\|_{0,R}^2 \lesssim \sum_{k=1}^{d} \sum_{S_\ell \in \mathcal{T}} \sum_{\xi \in \mathcal{F}_0(A_\ell^{k-1})} |A_\ell^{k-1}| \, \|\partial_{x_k} v(\xi, \cdot)\|_{0,B_\ell^{d-k+1}}^2 .$$

Now, $|A_\ell^{k-1}| = \prod_{l=1}^{k-1} h_{l,\ell_l} \simeq \prod_{l=1}^{k-1} w_{l,\xi_l}$ for each $\xi \in \mathcal{F}_0(A_\ell^{k-1})$, where the weights w_{l,ξ_l} are defined by the conditions

$$\sum_{\xi_l \in \mathcal{G}_l} v^2(\xi_l) w_{l,\xi_l} = \|\mathcal{I}_{\mathcal{G}_l} v\|_{0,I_l}^2 \qquad \forall v \in C^0(I_l) \ .$$

Then, the assertion follows from (6.29). □

7 Stage SE-CG $\to$ DFE-CG

We turn now to the second stage of our iterated auxiliary space preconditioner, namely the construction of a preconditioner for the conforming spectral-element problem introduced in Sect. 5. The new preconditioner will be based on an additional auxiliary space, comprised of globally continuous piecewise affine elements on conformingly matched dyadic meshes. The latter are associated with the LGL-grids used in the spectral-element discretization according to the construction mentioned in the previous section.

7.1 Definition of the ASM ingredients

The roles of the spaces V and $\tilde{V}$ appearing in the ASM (see Sect. 3) are now as follows. Let us set $V := V_\delta \cap H_0^1(\Omega)$, where V_δ is defined in (2.15), while $\tilde{V} := V_{h,D} \cap H_0^1(\Omega)$, where

$$V_{h,D} = \{v \in C^0(\overline{\Omega}) \ : \ \forall R \in \mathcal{R} \ , \ v_{|R} := v_R \in V_{h,D,p}(R)\} \ . \tag{7.1}$$

Note that since the dyadic grids are by construction nested, the trace spaces obtained by restricting $V_{h,D}$ to any interface of two adjacent elements are non-trivial. Also note that now $\tilde{V} \not\subset V$ so that the full ASM assumptions have to be checked.

Since all our finite dimensional spaces are contained in $H_0^1(\Omega)$ we set

$$\hat{a}(u,v) = \tilde{a}(u,v) = a(u,v) = (\nabla u, \nabla v)_{0,\Omega} = \sum_{R\in\mathcal{R}} (\nabla u, \nabla v)_{0,R} =: \sum_{R\in\mathcal{R}} a_R(u,v) \ .$$

We next have to specify the auxiliary form b. A central point of this section is the fact that we can no longer choose the form b as in Definition 5.1. In this original form it was designed to absorb the jump terms which are now missing. In the current situation it would therefore certainly ensure (3.3) but would actually be too strong an overestimation of the bilinear form a caused by using an inverse estimate on strongly anisotropic hyper-rectangles. As a consequence, one now runs into difficulties verifying the conditions (3.6) and (3.7). Our modifications are guided by the following closer look at the form a. The restriction $a_R(u,v)$ of $a(u,v)$ to any element $R = \times_{k=1}^d I_k$ is the sum of d bilinear forms, i.e., $a_R(u,v) = \sum_{k=1}^d a_{R,k}(u,v)$, where each form $a_{R,k}$ is the tensor product of univariate forms

$$a_{R,k}(u,v) = \int_R \partial_k u \partial_k v \, dx = \int_{R'_k} \left(\int_{I_k} \partial_k u \partial_k v \, dx_k \right) dx',$$

with $R'_k = \times_{\ell \neq k} I_\ell$.

The idea is to "weaken" the bilinear form b by avoiding the inverse estimates in regions where the LGL-grid is too anisotropic while preserving the validity of (3.3). Our ansatz for the form $b(u,v)$ follows the above structure of a, i.e., we set

$$b(u,v) = \sum_{R\in\mathcal{R}} b_R(u,v) \ , \qquad b_R(u,v) = \sum_{k=1}^d b_{R,k}(u,v). \tag{7.2}$$

Moreover, recall that for $v \in \mathbb{Q}_p(R)$ and $v_h := \mathcal{I}_{h,p}^R(v)$ our norm equivalences imply $a_{R,k}(v,v) \simeq a_{R,k}(v_h,v_h)$. Hence, it suffices to arrange that $a_{R,k}(v_h,v_h) \lesssim b_{R,k}(v,v)$. We proceed now defining

$b_{R,k}(u,v)$ in a cell-wise manner for any $u, v \in V + \tilde{V}$. To that end, we first decompose R into the d-dimensional LGL-subcells $S_\ell = S_\ell(R) = \times_{k=1}^{d} I_{k,\ell_k}$ for $\ell \in \times_{k=1}^{d}\{1,\ldots,p_k\}$, where $p = p(R)$ and each partition $\mathcal{T}_k(I_k) = \mathcal{T}(\mathcal{G}_{p_k}(I_k)) = \{I_{k,i} : 1 \le i \le p_k\}$ is generated by the LGL-grid $\mathcal{G}_{p_k}(I_k)$. Next, for each $1 \le k \le d$, we decompose the partition $\mathcal{T}(R) = \{S_\ell(R)\}$ of R into two parts $\mathcal{T}_k^{(0)}(R)$, $\mathcal{T}_k^{(1)}(R)$ defined as follows. Setting $h_{l,\ell_l} := |I_{l,\ell_l}|$ and fixing a constant $C_{\mathrm{aspect}} > 0$, we let

$$S_\ell \in \mathcal{T}_k^{(0)}(R) \quad \text{if} \quad \frac{\max_{l\neq k} h_{l,\ell_l}}{h_{k,\ell_k}} > C_{\mathrm{aspect}}, \qquad S_\ell \in \mathcal{T}_k^{(1)}(R) \text{ otherwise.} \tag{7.3}$$

Thus $\mathcal{T}_k^{(0)}(R)$ and $\mathcal{T}_k^{(1)}(R)$ are comprised of "strongly anisotropic" and "sufficiently isotropic" cells, respectively. In analogy to $a_{R,k}(u_h,v_h) = \sum_{S_\ell\in\mathcal{T}(R)} a_{R,k,S_\ell}(u_h,v_h)$ we make an ansatz for $b_{R,k}(u,v)$ as

$$b_{R,k}(u,v) = \sum_{S_\ell\in\mathcal{T}_k^{(0)}(R)} b_{R,k,S_\ell}^{(0)}(u,v) + \sum_{S_\ell\in\mathcal{T}_k^{(1)}(R)} b_{R,k,S_\ell}^{(1)}(u,v) \;=:\; b_{R,k}^{(0)}(u,v) + b_{R,k}^{(1)}(u,v)\ , \tag{7.4}$$

so that we still have $a_{R,k,S_\ell}(u_h,v_h) \lesssim b_{R,k,S_\ell}^{(i)}(u,v)$ for all $S_\ell \in \mathcal{T}_k^{(i)}(R)$, $i = 0,1$, as follows. In analogy to the factorization $R = I_k \times R_k'$, we define for every $S_\ell \in \mathcal{T}(R)$ the $(d-1)$-dimensional hyper-rectangle $S_{\ell,k}' := S_{\ell,k}'(R) := \times_{l=1,l\neq k}^{d} I_{l,\ell_l}$. The idea is to bound the terms

$$\int_{S_\ell} \partial_{x_k} u_h \partial_{x_k} v_h\, dx = \int_{S_{\ell,k}'} \left(\int_{I_{k,\ell_k}} \partial_{x_k} u_h(x_k,x')\partial_{x_k} v_h(x_k,x')\, dx_k \right) dx'$$

by using quadrature in all but the k-th variable while keeping the integral with respect to the k-th variable for $S_\ell \in \mathcal{T}_k^{(0)}(R)$, and applying an inverse estimate for $S_\ell \in \mathcal{T}_k^{(1)}(R)$. Specifically, using the tensorized trapezoidal rule for integration over $S_{\ell,k}'$, which is the finite-element lumped mass matrix approximation [15, (4.4.44) on p. 220], we define for $S_\ell \in \mathcal{T}_k^{(0)}(R)$

$$b_{R,k,S_\ell}^{(0)}(u,v) := \sum_{\xi'\in\mathcal{F}_0(S_{\ell,k}')} \omega_{\ell,k}' \int_{I_{k,\ell_k}} \partial_{x_k} u_h(x_k,\xi')\partial_{x_k} v_h(x_k,\xi')\, dx_k\ , \tag{7.5}$$

where the weight

$$\omega_{\ell,k}' = \prod_{l=1,l\neq k}^{d} h_{l,\ell_l} = \mathrm{vol}_{d-1}(S_{\ell,k}') \tag{7.6}$$

is equal to the $(d-1)$-dimensional volume of $S_{\ell,k}'$, and as before, $\mathcal{F}_0(S_{\ell,k}')$ is the set of all its vertices. Note that this set is isomorphic to $\mathcal{G}_{p(R)}(R) \cap (S_{\ell,k}' \times \{\xi\})$, where ξ denotes any endpoint of the interval $I_{k,\ell_k} = [\xi_{k,\ell_k}, \xi_{k,\ell_k+1}]$.

On the other hand, for each $S_\ell \in \mathcal{T}_k^{(1)}(R)$ we apply to each summand of (7.5) the inverse estimate

$$\int_{I_{k,\ell_k}} \left[\partial_{x_k} u_h(x_k,x')\right]^2 dx_k \le \frac{2}{h_{k,\ell_k}} \left[u_h^2(\xi_{k,\ell_k},x') + u_h^2(\xi_{k,\ell_k+1},x')\right],$$

which leads us to define for $S_\ell \in \mathcal{T}_k^{(1)}(R)$

$$b_{R,k,S_\ell}^{(1)}(u,v) := \sum_{\xi'\in\mathcal{F}_0(S_{\ell,k}')} \sum_{\xi\in\mathcal{F}_0(I_{k,\ell_k})} c_{\xi,\xi'} \frac{\omega_{\ell,k}'}{h_{k,\ell_k}}\, u_h(\xi,\xi')\, v_h(\xi,\xi')\ , \tag{7.7}$$

where as before the $c_{\xi,\xi'}$ are tuning constants of order one which have to be chosen judiceously in practical applications. To simplify the exposition we shall suppress them in what follows.

In summary, we have

$$b(u,v) = \sum_{R\in\mathcal{R}} \sum_{k=1}^{d} \Big(\sum_{S_\ell \in \mathcal{T}_k^{(0)}(R)} b^{(0)}_{R,k,S_\ell}(u,v) + \sum_{S_\ell \in \mathcal{T}_k^{(1)}(R)} b^{(1)}_{R,k,S_\ell}(u,v) \Big), \tag{7.8}$$

where $b^{(i)}_{R,k,S_\ell}(u,v)$, $i = 0,1$, are defined by (7.5), (7.7), respectively. By construction this bilinear form satisfies the ASM condition (3.3).

Property 7.1. *One has*

$$a(v,v) \lesssim b(v,v) \qquad \forall v \in V\ . \tag{7.9}$$

Note that the relation (7.9) can be viewed as an *inverse estimate.*

Let us define next the operators Q and $\tilde{Q}$, starting with the former one. Obviously, this can be done element-wise, so let us fix again an element $R \in \mathcal{R}$. Given any $\tilde{v} \in \tilde{V}$, let us set $\tilde{v}_R := \tilde{v}_{|R} \in V_{h,D,p}(R)$. Let us denote for any vertex $z \in \mathcal{F}_0(R)$ of R by

$$\{E_1, E_2, \ldots, E_d\} = \mathcal{F}_1(z) \cap \mathcal{F}_1(R)$$

the set of edges of R containing z, with E_k parallel to the k-th coordinate direction. Let us also introduce the vector of polynomial degrees

$$p_z^* = (p^\sharp(E_1), p^\sharp(E_2), \ldots, p^\sharp(E_d)) \in \mathbb{N}^d$$

and note that, by definition of $p^\sharp(E_k)$ (recall (5.8)), we have $p_z^* \leq p(R)$ componentwise. Finally, let us introduce the localizing function $\Phi_z \in \mathbb{Q}_1(R)$, defined by the conditions $\Phi_z(y) = \delta_{y,z}$ for all $y \in \mathcal{F}_0(R)$. Then, we set

$$\tilde{v}_z^* := \mathcal{I}^R_{h,D,p_z^*}(\Phi_z \tilde{v}_R) \in V_{h,D,p_z^*}(R) \qquad \text{and} \qquad v_z^* = \mathcal{I}^R_{p_z^*}\, \tilde{v}_z^* \in \mathbb{Q}_{p_z^*}(R)\ . \tag{7.10}$$

Summing-up over the vertices of R, we define

$$\tilde{v}_R^* := \sum_{z\in\mathcal{F}_0(R)} \tilde{v}_z^* \in V_{h,D,p}(R) \qquad \text{and} \qquad Q_R \tilde{v}_R := v_R^* := \sum_{z\in\mathcal{F}_0(R)} v_z^* \in \mathbb{Q}_p(R)\ . \tag{7.11}$$

The following properties will be useful in the sequel.

Property 7.2. *For any edge $E \in \mathcal{F}_1(R)$, one has*

$$(\tilde{v}_R^*)_{|E} = (\tilde{v}_R)_{|E}\ .$$

Proof. If E has vertices z_1 and z_2, then

$$\big(\tilde{v}_{z_1}^* + \tilde{v}_{z_2}^*\big)_{|E} = \mathcal{I}^E_{h,D,p^\sharp(E)}\,((\Phi_{z_1} + \Phi_{z_2})\tilde{v}_R)_{|E} = \mathcal{I}^E_{h,D,p^\sharp(E)}\,(\tilde{v}_R)_{|E} = (\tilde{v}_R)_{|E}$$

since by continuity $(\tilde{v}_R)_{|E} \in V_{h,D,p^\sharp(E)}(E)$; on the other hand, $(\tilde{v}_y^*)_{|E} = 0$ for all $y \in \mathcal{F}_0(R)\setminus\{z_1,z_2\}$. Thus, $(\tilde{v}_R^*)_{|E} = \big(\tilde{v}_{z_1}^* + \tilde{v}_{z_2}^*\big)_{|E} = (\tilde{v}_R)_{|E}$. □

Property 7.3. *For any interface $F \in \mathcal{F}_{d-1}$, with $\mathcal{R}(F) = \{R', R''\}$, one has*

$$(\tilde{v}_{R'}^*)_{|F} = (\tilde{v}_{R''}^*)_{|F} \qquad \textit{and} \qquad (v_{R'}^*)_{|F} = (v_{R''}^*)_{|F}\ .$$

Proof. Let $\mathcal{F}_0(F) = \mathcal{F}_0(R') \cap \mathcal{F}_0(R'')$ be the set of vertices of F. Since, by continuity of $\tilde{v}$, $\tilde{v}_F := (\tilde{v}_{R'})_{|F} = (\tilde{v}_{R''})_{|F}$, one has $\left(\Phi_z \tilde{v}_{R'}\right)_{|F} = \Phi_z^F \tilde{v}_F = \left(\Phi_z \tilde{v}_{R''}\right)_{|F}$, $z \in \mathcal{F}_0(F)$, where $\Phi_z^F \in \mathbb{Q}_1(F)$ satisfies $\Phi_z^F(y) = \delta_{y,z}$ for all $y \in \mathcal{F}_0(F)$. Hence, denoting by $q_z^* = (p_z^*)' \in \mathbb{N}^{d-1}$ the reduced degree vector obtained from p_z^* by dropping the component in the direction orthogonal to F, one concludes that

$$
\begin{aligned}
(\tilde{v}_{R'}^*)_{|F} &= \sum_{z \in \mathcal{F}_0(F)} \mathcal{I}_{h,D,q_z^*}^F \left(\Phi_z \tilde{v}_{R'}\right)_{|F} = \sum_{z \in \mathcal{F}_0(F)} \mathcal{I}_{h,D,q_z^*}^F \left(\Phi_z^F \tilde{v}_F\right) \\
&= \sum_{z \in \mathcal{F}_0(F)} \mathcal{I}_{h,D,q_z^*}^F \left(\Phi_z \tilde{v}_{R''}\right)_{|F} = (\tilde{v}_{R''}^*)_{|F} \ ,
\end{aligned}
$$

where we have used that q_z^* is the same for both R' and R''. This confirms the first part of the assertion. Abbreviating $\tilde{v}_z^F := \mathcal{I}_{h,D,q_z^*}^F \left(\Phi_z^F \tilde{v}_F\right)$, the second one follows from

$$
(v_{R'}^*)_{|F} = \sum_{z \in \mathcal{F}_0(F)} \mathcal{I}_{q_z^*}^F \, \tilde{v}_z^F = (v_{R''}^*)_{|F} \ ,
$$

which completes the proof. $\square$

The previous property guarantees interelement continuity of the functions $\tilde{v}_R^*$ and v_R^*, justifying the following definition of the operator Q.

Definition 7.4. *Let $Q : \tilde{V} \to V$ be given by*

$$
(Q\tilde{v})_{|R} = Q_R \tilde{v}_R = v_R^* \qquad \forall R \in \mathcal{R} \qquad \forall \tilde{v} \in \tilde{V} \ ,
$$

where v_R^* is defined in (7.11).

The definition of the operator $\tilde{Q}$ follows the same lines as above. Given any $v \in V$ and any $R \in \mathcal{R}$, we set $v_R = v_{|R} \in \mathbb{Q}_p(R)$. Then, the chain (7.10)-(7.11) is replaced by the following one:

$$
v_z^* := \mathcal{I}_{p_z^*}^R \left(\Phi_z v_R\right) \in \mathbb{Q}_{p_z^*}(R) \qquad \text{and} \qquad \tilde{v}_z^* := \mathcal{K}_{h,D,p_z^*}^R \, v_z^* \in V_{h,D,p_z^*}(R) \ . \tag{7.12}
$$

Summing over the vertices of R, we define

$$
v_R^* := \sum_{z \in \mathcal{F}_0(R)} v_z^* \in \mathbb{Q}_p(R) \qquad \text{and} \qquad \tilde{Q}_R v_R := \tilde{v}_R^* = \sum_{z \in \mathcal{F}_0(R)} \tilde{v}_z^* \in V_{h,D,p}(R) \ . \tag{7.13}
$$

As above, one easily confirms interelement continuity, which suggests the following definition.

Definition 7.5. *The operator $\tilde{Q} : V \to \tilde{V}$ is given by*

$$
(\tilde{Q}v)_{|R} := \tilde{Q}_R v_R = \tilde{v}_R^* \qquad \forall R \in \mathcal{R} \qquad \forall v \in V \ ,
$$

where $\tilde{v}_R^*$ is defined in (7.13).

7.2 Check of the ASM assumptions for Q and $\tilde{Q}$

Hereafter, we deal with the ASM conditions (3.5) and (3.7) involving the operator Q, as well as (3.4) and (3.6) involving the operator $\tilde{Q}$

Proposition 7.6. *The operator Q is linear and satisfies the continuity assumption* (3.5).

Proof. We have to prove that $|Q\tilde v|_{1,\Omega} \lesssim |\tilde v|_{1,\Omega}$ for all $\tilde v \in \tilde V$. This follows if, for any $R \in \mathcal{R}$, we prove that

$$|v_R^*|_{1,R} \lesssim |\tilde v_R|_{1,R} \qquad \forall \tilde v_R \in V_{h,D,p}(R) \ . \tag{7.14}$$

A classical mapping-and-scaling argument in Finite Element analysis tells us that this result holds provided it holds when R is the reference element $\hat R = \times_{k=1}^d \hat I$, with $\hat I = [-1,1]$. For this element, it is enough to prove that

$$|v^*|_{1,\hat R} \lesssim \|\tilde v\|_{1,\hat R} \qquad \forall \tilde v \in V_{h,D,p}(\hat R) \ . \tag{7.15}$$

Indeed, changing $\tilde v$ into $\tilde v + c$, by any $c \in \mathbb{R}$, does not change the left-hand side, whence

$$|v^*|_{1,\hat R} \lesssim \inf_{c\in\mathbb{R}} \|\tilde v + c\|_{1,\hat R} \lesssim |\tilde v|_{1,\hat R} \ .$$

In order to establish (7.15), let us first consider a univariate function $\tilde v \in V_{h,D,p}(\hat I)$ and let Φ denote the affine function taking the value 1 at one endpoint of the interval and 0 at the other one. Let us prove that if $cp \le q \le p$ for some fixed constant $c > 0$, one has

$$|\mathcal{I}_{h,D,q}(\Phi\tilde v)|_{m,\hat I} \lesssim \|\tilde v\|_{m,\hat I} \ , \qquad m = 0, 1 \ , \tag{7.16}$$

where, of course, the involved constant depends on the proportionality factor c. For $m = 0$, we have

$$\|\mathcal{I}_{h,D,q}(\Phi\tilde v)\|_{0,\hat I}^2 \lesssim \sum_{\zeta\in\mathcal{G}_{D,q}(\hat I)} (\Phi(\zeta)\tilde v(\zeta))^2 h_{D,q}(\zeta) \lesssim \sum_{\eta\in\mathcal{G}_{D,p}(\hat I)} \tilde v(\eta)^2 h_{D,p}(\eta) \lesssim \|\tilde v\|_{0,\hat I}^2 \ ,$$

since $\Phi^2 \le 1$ and $h_{D,q}(\zeta) \lesssim h_{D,p}(\zeta)$ for all $\zeta \in \mathcal{G}_{D,q}(\hat I) \subseteq \mathcal{G}_{D,p}(\hat I)$. For $m = 1$, we have by Lemma 6.7,

$$|\mathcal{I}_{h,D,q}(\Phi\tilde v)|_{1,\hat I} \lesssim |\Phi\tilde v|_{1,\hat I} \lesssim \|\tilde v\|_{1,\hat I},$$

where the last inequality holds since we are working on the reference element. Hence, (7.16) is proven. Using this result and Proposition 6.14, we obtain the bound

$$|\tilde v_z^*|_{1,\hat R} \lesssim \|\tilde v\|_{1,\hat R}$$

for each function $\tilde v_z^*$ defined as in (7.10) on $\hat R$. Then, Property 6.17 yields $|v_z^*|_{1,\hat R} \lesssim \|\tilde v\|_{1,\hat R}$, and (7.15) follows by the triangle inequality, since $|\mathcal{F}_0(\hat R)| \simeq 1$. ☐

Proposition 7.7. *The operator Q satisfies the Jackson condition* (3.7)*, i.e., one has*

$$b(\tilde v - Q\tilde v, \tilde v - Q\tilde v) \lesssim |\tilde v|_{1,\Omega}^2 \qquad \forall \tilde v \in \tilde V \ ,$$

where the multiplicative constant in the above estimate depends on the constant C_{aspect} in (7.3).

Proof. For each $R \in \mathcal{R}$ and each $k = 1, \dots, d$, let us recall the definitions (7.4), (7.5) and (7.7) of the form $b_{R,k}(u,v)$ and its portions $b_{R,k}^{(0)}(u,v)$ and $b_{R,k}^{(1)}(u,v)$. Concerning the former portion, observe that

$$\begin{aligned} b_{R,k}^{(0)}(v,v) &= \sum_{S_\ell\in\mathcal{T}_k^{(0)}(R)} \sum_{\xi'\in\mathcal{G}(S'_{\ell,k})} \omega'_{\ell,k} \int_{I_{k,\ell_k}} \left|\partial_{x_k}\mathcal{I}_{h,p}^R v(\xi',x_k)\right|^2 dx_k \\ &\simeq \sum_{S_\ell\in\mathcal{T}_k^{(0)}(R)} \int_{S_\ell} \left|\partial_{x_k}\mathcal{I}_{h,p}^R v(x)\right|^2 dx \le \sum_{S_\ell\in\mathcal{T}(R)} \int_{S_\ell} \left|\partial_{x_k}\mathcal{I}_{h,p}^R v(x)\right|^2 dx \le |\mathcal{I}_{h,p}^R v|_{1,R}^2 \ , \end{aligned} \tag{7.17}$$

where we have used the uniform equivalence of the weights $\omega'_{\ell,k}$ (see (7.6)) with the integration weights for multi-linear functions on the cell $S'_{\ell,k}$. Thus, for all $\tilde v_R \in V_{h,D,p}(R)$, we have

$$\begin{aligned} b_{R,k}^{(0)}(\tilde v_R - Q_R\tilde v_R, \tilde v_R - Q_R\tilde v_R) &\lesssim |\mathcal{I}_{h,p}^R(\tilde v_R - Q_R\tilde v_R)|_{1,R}^2 \\ &\lesssim |\mathcal{I}_{h,p}^R(\tilde v_R)|_{1,R}^2 + |\mathcal{I}_{h,p}^R(Q_R\tilde v_R)|_{1,R}^2 \lesssim |\tilde v_R|_{1,R}^2 \ , \end{aligned} \tag{7.18}$$

where the last bound follows immediately from Lemma 6.8, Properties 6.11 and 6.16, and Proposition 7.6.

Consider now the portion $b^{(1)}_{R,k}(u,v)$. Arguing as above, one has

$$b^{(1)}_{R,k}(v,v) = \sum_{S_\ell \in \mathcal{T}^{(1)}_k(R)} \sum_{\xi' \in \mathcal{G}(S'_{\ell,k})} \omega'_{\ell,k} \sum_{\xi \in \mathcal{G}(I_{k,\ell_k})} h^{-1}_{k,\ell_k} \, |\mathcal{I}^R_{h,p} v(\xi',\xi)|^2 \simeq \sum_{S_\ell \in \mathcal{T}^{(1)}_k(R)} \int_{S_\ell} h^{-2}_{k,\ell_k} \, |\mathcal{I}^R_{h,p} v(x)|^2 \, dx \, .$$

Now observe that, by definition of $\mathcal{T}^{(1)}_k(R)$ (see (7.3)), one has $h_{k,\ell_k} \geq \max(1, C^{-1}_{\text{aspect}})\, h_\ell$, with $h_\ell = \max_l h_{l,\ell_l}$. Hence,

$$\begin{aligned} b^{(1)}_{R,k}(v,v) &\lesssim \sum_{S_\ell \in \mathcal{T}^{(1)}_k(R)} \int_{S_\ell} h_\ell^{-2} \, |\mathcal{I}^R_{h,p} v(x)|^2 \, dx \leq \sum_{S_\ell \in \mathcal{T}(R)} \int_{S_\ell} h_\ell^{-2} \, |\mathcal{I}^R_{h,p} v(x)|^2 \, dx \\ &= \|h^{-1} \mathcal{I}^R_{h,p} v\|^2_{0,R} \lesssim \|h^{-1}(v - \mathcal{I}^R_{h,p} v)\|^2_{0,R} + \|h^{-1} v\|^2_{0,R} \, , \end{aligned}$$

where $h = \sum_\ell h_\ell \chi_{S_\ell}$ is the LGL meshsize function in R. If $\tilde v_R \in V_{h,D,p}(R)$, this yields

$$\begin{aligned} b^{(1)}_{R,k}(\tilde v_R - Q_R \tilde v_R, \tilde v_R - Q_R \tilde v_R) &\lesssim \|h^{-1}(\tilde v_R - \mathcal{I}^R_{h,p} \tilde v_R)\|^2_{0,R} + \|h^{-1}(Q_R \tilde v_R - \mathcal{I}^R_{h,p}(Q_R \tilde v_R))\|^2_{0,R} \\ &\quad + \|h^{-1}(\tilde v_R - Q_R \tilde v_R)\|^2_{0,R} \, . \end{aligned} \tag{7.19}$$

Now we invoke Proposition 6.19, with different choices of the grid $\mathcal{G}$ and the space W, to bound each of the three summands on the right-hand side. For the first summand, we have $\mathcal{G} = \mathcal{G}_p(R)$ (the LGL-grid of order p in R) and $W = V_{h,D,p}(R)$. We note that, due to Lemma 6.8, the bounds (6.29) are satisfied with $\bar c_k \lesssim 1$. Thus we get

$$\|h^{-1}(\tilde v_R - \mathcal{I}^R_{h,p} \tilde v_R)\|^2_{0,R} \lesssim |\tilde v_R|^2_{1,R} \, . \tag{7.20}$$

For the second summand, we recall that $Q_R \tilde v_R \in \mathbb{Q}_p(R)$, so that we have again $\mathcal{G} = \mathcal{G}_p(R)$, whereas now $W = \mathbb{Q}_p(R)$. The bounds (6.29) are now satisfied with $\bar c_k \lesssim 1$ because of Property 6.11. Thus, recalling (7.14), we obtain

$$\|h^{-1}(Q_R \tilde v_R - \mathcal{I}^R_{h,p}(Q_R \tilde v_R))\|^2_{0,R} \lesssim |Q_R \tilde v_R|^2_{1,R} \lesssim |\tilde v_R|^2_{1,R} \, . \tag{7.21}$$

At last, we bound the third summand on the right-hand side of (7.19). To this end, recalling the definition (7.11) of $Q_R \tilde v$, noting that $\tilde v_R = \sum_{z \in \mathcal{F}_0(R)} \Phi_z \tilde v_R$, and defining $\tilde v_z := \Phi_z \tilde v_R$, $z \in \mathcal{F}_0(R)$, it suffices to bound the quantity $\|h^{-1}(\tilde v_z - \mathcal{I}^R_{p^*_z}(\mathcal{I}^R_{h,D,p^*_z} \tilde v_z))\|^2_{0,R}$ for each $z \in \mathcal{F}_0(R)$. Writing

$$\tilde v_z - \mathcal{I}^R_{p^*_z}(\mathcal{I}^R_{h,D,p^*_z} \tilde v_z) = (\tilde v_z - \mathcal{I}^R_{h,D,p^*_z} \tilde v_z) + (\mathcal{I}^R_{h,D,p^*_z} \tilde v_z - \mathcal{I}^R_{p^*_z}(\mathcal{I}^R_{h,D,p^*_z} \tilde v_z)),$$

and setting for simplicity $\tilde w_z = \mathcal{I}^R_{h,D,p^*_z} \tilde v_z \in V_{h,D,p^*}(R)$, we have

$$\|h^{-1}(\tilde v_z - \mathcal{I}^R_{p^*_z}(\mathcal{I}^R_{h,D,p^*_z} \tilde v_z))\|^2_{0,R} \lesssim \|h^{-1}(\tilde v_z - \mathcal{I}^R_{h,D,p^*_z} \tilde v_z))\|^2_{0,R} + \|h^{-1}(\tilde w_z - \mathcal{I}^R_{p^*_z} \tilde w_z)\|^2_{0,R} \, . \tag{7.22}$$

We now proceed as in the proof of Proposition 7.6, i.e., we work on the reference element $\hat R$ viewed as an affine image of R. This simplifies handling the factor Φ_z when eventually bounding the H^1-seminorm of $\tilde v_z = \Phi_z \tilde v_R$ by that of $\tilde v_R$ on the element R.

We want to apply Proposition 6.19 to the first summand on the right-hand side of (7.22), with $\mathcal{G} = \mathcal{D}_{p^*}(\hat R)$ (the dyadic grid of order p^* in $\hat R$) and $W = \Phi_z V_{h,D,p^*}(\hat R)$. To this end, we observe that the meshsize function h associated with the grid $\mathcal{G}_p(\hat R)$, as a consequence of Corollary 6.6, is uniformly comparable to the meshsize function h_{D,p^*} associated with the grid $\mathcal{D}_{p^*}(\hat R)$, i.e., $h \simeq h_{D,p^*}$ pointwise in $\hat R$. On the other hand, the bounds (6.29) are satisfied with $\bar c_k \lesssim 1$; this easily follows from the fact that the restriction of $\tilde{v}_z$ to any cell of the grid $\mathcal{D}_{p^*}(\hat{R})$ is a piecewise multi-quadratic function belonging to a finite dimensional space whose dimension is bounded independently of p. Thus, we obtain

$$\|h^{-1}(\tilde{v}_z - \mathcal{I}^{\hat{R}}_{h,D,p^*_z}\tilde{v}_z))\|^2_{0,\hat{R}} \lesssim |\tilde{v}_z|^2_{1,\hat{R}} \lesssim \|\tilde{v}_{\hat{R}}\|^2_{1,\hat{R}} \,. \tag{7.23}$$

The second summand on the right-hand side of (7.22) can be bounded with the aid of Proposition 6.19 as well. Indeed, using the property that $\mathcal{I}_{h,q}(\mathcal{I}_q v) = \mathcal{I}_{h,q} v$ if $\mathcal{I}_{h,q} v$ and $\mathcal{I}_q v$ are the low- and high-order interpolants of a continuous function on the same grid, one has

$$v - \mathcal{I}_q v = v - \mathcal{I}_{h,q}(\mathcal{I}_q v) + \mathcal{I}_{h,q}(\mathcal{I}_q v) - \mathcal{I}_q v = (v - \mathcal{I}_{h,q} v) - (\mathcal{I}_q v - \mathcal{I}_{h,q}(\mathcal{I}_q v)) \,.$$

In our situation, this yields with $\tilde{u}_z = \mathcal{I}^{\hat{R}}_{p^*_z}\tilde{w}_z \in \mathbb{Q}_{p^*}(\hat{R})$

$$\|h^{-1}(\tilde{w}_z - \mathcal{I}^{R}_{p^*_z}\tilde{w}_z)\|^2_{0,\hat{R}} \lesssim \|h^{-1}(\tilde{w}_z - \mathcal{I}^{\hat{R}}_{h,p^*_z}\tilde{w}_z)\|^2_{0,\hat{R}} + \|h^{-1}(\tilde{u}_z - \mathcal{I}^{\hat{R}}_{h,p^*_z}\tilde{u}_z)\|^2_{0,\hat{R}} \,.$$

so that we can apply Proposition 6.19 with $\mathcal{G} = \mathcal{G}_{p^*}(\hat{R})$ and either $W = V_{h,D,p}(\hat{R})$ or $W = \mathbb{Q}_{p^*}(\hat{R})$. Again, the function h is uniformly comparable to the function h_{p^*} associated with the grid $\mathcal{G}_{p^*}(\hat{R})$, and one easily checks that the bounds (6.29) are satisfied with $\bar{c}_k \lesssim 1$ with both choices of W. Thus,

$$\|h^{-1}(\tilde{w}_z - \mathcal{I}^{\hat{R}}_{p^*_z}\tilde{w}_z)\|^2_{0,\hat{R}} \lesssim |\tilde{w}_z|^2_{1,\hat{R}} \lesssim |\tilde{v}_z|^2_{1,\hat{R}} \lesssim \|\tilde{v}_{\hat{R}}\|^2_{1,\hat{R}} \,, \tag{7.24}$$

where the second inequality follows from Lemma 6.8 and Property 6.16. Going back to the element R, the bounds (7.22), (7.23) and (7.24) imply

$$\|h^{-1}(\tilde{v}_z - \mathcal{I}^{R}_{p^*_z}(\mathcal{I}^{R}_{h,D,p^*_z}\tilde{v}_z))\|^2_{0,R} \lesssim |\tilde{v}_R|^2_{1,R} \,,$$

which, together with (7.20) and (7.21), allows us to obtain from (7.19)

$$b^{(1)}_{R,k}(\tilde{v}_R - Q_R\tilde{v}_R, \tilde{v}_R - Q_R\tilde{v}_R) \lesssim |\tilde{v}_R|^2_{1,R} \,.$$

This completes the proof of Proposition 7.7. □

In a similar manner as above, one can check the ASM assumptions for $\tilde{Q}$, where essentially the order of the operators $\mathcal{I}_p, \mathcal{I}_{h,D,p}$ is interchanged. However, Lemma 6.8 allows us to argue as before.

Proposition 7.8. *The operator $\tilde{Q}$ satisfies the continuity assumption* (3.4) *and the Jackson assumption* (3.6)*.*

So far we have shown that the above choice of auxiliary spaces complies with the ASM requirements so that, in principle, the stage II preconditioner is again optimal. However, again it remains to precondition the new auxiliary problem, i.e., to identify $\mathbf{C}_{\tilde{\mathbf{A}}}$. As the auxiliary space $\tilde{V}$ now corresponds to a hierarchy of nested low order finite element spaces, this task looks more feasible. Nevertheless, the strong anisotropy appearing in the underlying dyadic meshes poses a further obstruction. In fact, an asymptotically optimal treatment that works for arbitrary degrees seems to preclude the application of standard tools. Therefore, we postpone this issue to the forthcoming part II of this work where a multi-wavelet preconditioner will be proposed and analyzed. Here we address in the following section a second obstruction, namely the fact that the Gramian $\mathbf{B}$ associated with the auxiliary form b, defined by (7.8), is no longer diagonal, due to the coupling across element interfaces and the remaining integrals of derivatives in strongly anisotropic grid areas.

8 Numerical results

In this section we quantify the performance of the multi-stage preconditioner, examining first the influence of the various ingredients in each of the two stages discussed in this paper. This includes the resulting condition numbers and their dependence on the parameters, in particular on the polynomial degrees. In the experiments the condition numbers are obtained as quotient of the largest and smallest eigenvalue of the preconditioned linear systems of equations. Since the matrices involved are large and sparse, we apply a Jacobi-Davidson type method for the eigenvalue computation that is tailored to the specific needs in this application, see [9] for details.

8.1 Test cases

We now consider two test scenarios that represent typical situations involving varying polynomial degrees when solving a Poisson problem (2.13) on the domain $\Omega = [0,3]^2 \subset \mathbb{R}^2$ that is divided into nine square patches of equal size as depicted in Fig. 2(a). This grid of 3×3 patches contains the central patch that is not in contact with the domain boundary. Inside each patch we use at this point just constant degree vectors, i.e., the polynomial degrees are the same in x- and y-direction inside each patch. However, the polynomial degree may vary from patch to patch and we are interested in quantifying the influence of patchwise varying polynomial degrees on the performance of our preconditioning technique.

In this first test scenario we arrange the polynomial degrees in the nine patches to be either p or q in a checkerboard-style pattern. Concerning the values of $p, q \in \mathbb{N}$, we consider the following five cases: (i) we either use constant polynomial degree $q = p$, (ii) simulate a small variation of the degree by choosing $q = p + 2$, or a large variation of the degree represented by multiplicative relations (iii) $q = 3/2p$ for even p, (iv) $q = 7/4p$ for p chosen as a multiple of 4 or (v) $q = 2p$.

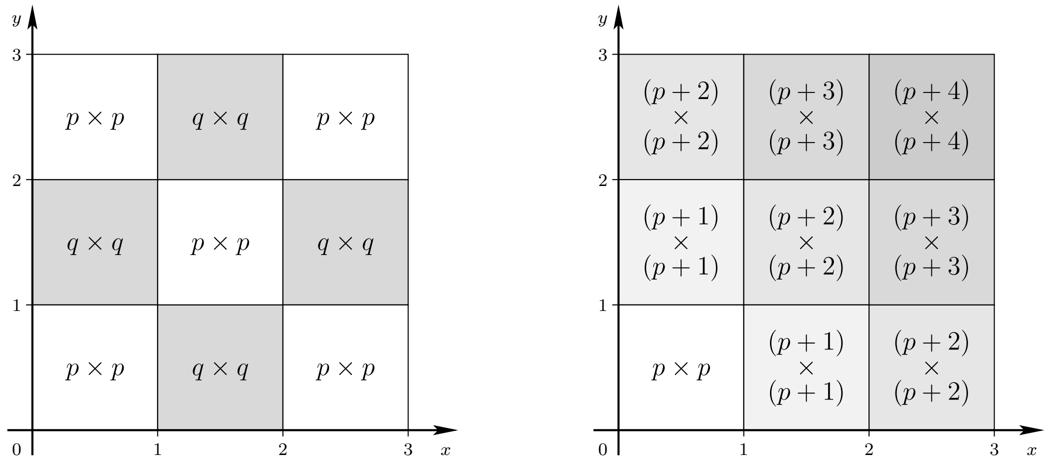

(a) First test scenario: checkerboard-style grid.

(b) Second test scenario.

Figure 2: Grid and distribution of polynomial degrees for the test scenarios. Darker shading indicates higher polynomial degree in the patch.

In the second scenario we simulate a situation that typically arises in p-adaptation towards a singularity, namely we solve Poisson's equation (2.13) on Ω again split into 3×3 square patches. Assuming a singularity located at the origin, the polynomial degree increases in directions away from the singularity as illustrated in Fig. 2(b).

8.2 Stage SE-DG $\to$ SE-CG

In the first stage, we apply the auxiliary space method to precondition the DG-spectral element problem by an auxiliary problem given by a conforming Galerkin formulation. We first investigate the resulting condition numbers and their dependence on the polynomial degrees for that stage only, i.e., the auxiliary problem is solved exactly.

8.2.1 Choice of the bilinear form $b(\cdot,\cdot)$

In Subsect. 5.2 the auxiliary bilinear form b in the first ASM stage is defined up to "tuning" constants $c_\xi \sim 1$ that still need to be specified for $\xi \in \mathcal{G}_p(R)$, $R \in \mathcal{R}$. In view of the inverse estimate used in the proof of Proposition 5.6, we define $b_\delta : V_\delta \times V_\delta \to \mathbb{R}$ as

$$b_\delta(u,v) = \beta_1 \left(c_1^2 \sum_{R\in\mathcal{R}} \sum_{\xi\in\mathcal{G}_p(R)} u(\xi)\, v(\xi)\, W_\xi + \gamma\rho_1 \sum_{F\in\mathcal{F}_{d-1}} \omega_F \sum_{\pm} \sum_{\xi\in\mathcal{G}_p(F,R^\pm)} w_{F,R^\pm} u^\pm(\xi) v^\pm(\xi) \right),$$

where $w_{F,R^\pm}$ is the LGL quadrature weight on F seen as face of $R^\pm$. Consequently, a reasonable ansatz for the constants c_ξ in (5.7) is

$$c_\xi = \begin{cases} \beta_1(c_1^2 + \gamma\rho_1\omega_F w_{F,R}/W_\xi), & \text{for } \xi \in \mathcal{G}_p(F,R),\ F \in \mathcal{F}_{d-1}(R),\ R \in \mathcal{R}, \\ \beta_1 c_1^2, & \text{else.} \end{cases}$$

Preliminary experiments concerning the constant arising in the inverse estimate reveal that $c_1^2 = 10$ is a good choice which we fix in our subsequent tests.

We emphasize that with this choice of b the corresponding matrix $\mathbf{B}$ is diagonal for any choice of $\beta_1 > 0$ and $\rho_1 \geq 0$, i.e., the complexity of solving a linear system with the matrix $\mathbf{B}$ is proportional to the number of unknowns.

8.2.2 Optimal choice of the parameters β_1 and ρ_1

We next address the question of suitably specifying the parameters β_1 and ρ_1 in the bilinear form b. In particular, is there a good choice for these parameters that works by and large independently of other parameters, such as the polynomial degree? We investigate this problem for the first test scenario and and the (extreme) case (v) $q = 2p$. The condition numbers $\kappa_{\mathrm{ASM}} = \kappa(\mathbf{C_A A})$ of the linear system of equations preconditioned by the auxiliary space method, where the auxiliary problem is solved exactly are depicted for $p = 8$ and for $p = 16$ in Fig. 3 as functions of $\beta_1 \in [0.05, 1.1]$ and $\rho_1 \in [0, 2]$; contour plots, i.e. the lines of constant condition number, are displayed.

We observe that the simple choice $\beta_1 = 1$ and $\rho_1 = 0$, which is $c_\xi = 1$, is not optimal. In fact, for both $p = 8$ and $p = 16$ there is a very flat minimum of the condition number that is located near the parameter point $(\beta_1, \rho_1) = (0.15, 1.25)$. From now on we fix these parameter values for the rest of the paper.

8.2.3 Dependence on the polynomial degrees

Now we are ready to investigate the key issue, namely the robustness of the preconditioner with respect to the polynomial degrees. Fig. 4(a) shows the condition numbers obtained in the first scenario for the relations (i) - (v) between p and q. We observe that the condition numbers stay uniformly bounded as p increases although the upper bound depends on the ratio q/p. In the case of additively increasing the polynomial degree $q = p + 2$, the quotient q/p decreases which is also visible in Fig. 4(a).

The analogous plot for the second test scenario, representing a typical p-adaptation, is depicted in Fig. 4(b). In the second test scenario the condition numbers are almost constant and slightly smaller than 7.5.

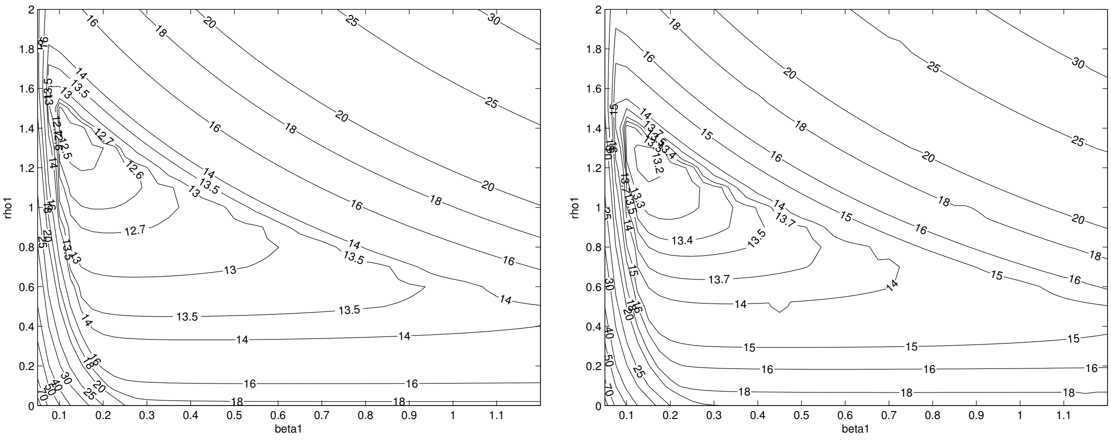

(a) $p = 8$, $q = 16$ (b) $p = 16$, $q = 32$

Figure 3: Contour plots illustrating the dependence of the condition number $\kappa_{\mathrm{ASM}} = \kappa(\mathbf{C_A A})$ on $\beta_1 > 0$ and $\rho_1 \geq 0$.

8.3 Stage SE-CG $\rightarrow$ DFE-CG

Now we analyze the performance of the preconditioner in the second stage.

8.3.1 Solution of the smoothing problem

Every application of the auxiliary space preconditioner in the second stage requires solving two linear systems of equations: the auxiliary problem involving the matrix $\tilde{\mathbf{A}}$ and the problem involving the matrix $\mathbf{B}$, which we call the smoothing problem. Unfortunately, the corresponding matrix $\mathbf{B} = \mathbf{B}_2$ in the second stage is in general no longer diagonal. The modifications on the strongly anisotropic cells in $\mathcal{T}_k^{(0)}(R)$, $R \in \mathcal{R}$, cause a slightly stronger coupling than for a purely diagonal structure although $\mathbf{B}_2$ remains diagonal in the bulk of the element. We therefore need an efficient solution for the smoothing problem as well. We first consider the case where the domain consists of a single patch since this already offers valuable insight into various effects.

Single patch: sparsity pattern and reordering Regarding the possible use of both (blockwise) direct or iterative solvers, we first study the sparsity pattern of $\mathbf{B}_2$ obtained when the polynomial Lagrange nodal basis is ordered in a line-wise fashion. In particular, since the Lagrange nodal basis functions with reference nodes at the boundary of the patch need a special treatment anyway, we are interested in the sparsity pattern of the submatrix for ansatz functions in the bulk of the patch. In Fig. 5(a) this is depicted for a patch with polynomial degree $p = 25$ in both directions. We confine the discussion in this paper to the bivariate case $d = 2$.

Since the cells of high anisotropy are selected on a per-subcell basis the inverse estimate is used wherever possible. Therefore, $\mathbf{B}_2$ is still very sparse. The two bilinear forms $b^{(1)}_{R,1,S_\ell}$ and $b^{(1)}_{R,2,S_\ell}$, see (7.5) and (7.7) for their definitions, contribute only to the main diagonal of the matrix. Since a rectangular cell in two spatial dimensions can only be anisotropic in at most one direction for $C_{\mathrm{aspect}} > 1$ the intersection of the regions where $b^{(0)}_{R,1,S_\ell}$ and $b^{(0)}_{R,2,S_\ell}$ are applied does not contain a subcell. At most this intersection might be comprised of isolated nodes. Because of the quasi-uniformity of LGL-grids the regions $\mathcal{T}_1^{(0)}(R)$ and $\mathcal{T}_2^{(0)}(R)$ do not overlap if C_{aspect} is large enough, see e.g. [8, 9].

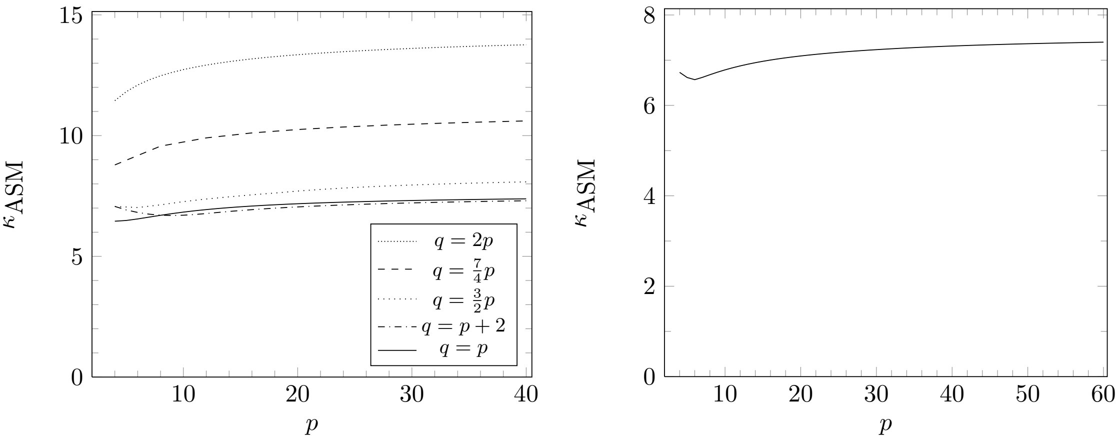

(a) First test scenario. (b) Second test scenario.

Figure 4: Condition numbers $\kappa_{\mathrm{ASM}} = \kappa(\mathbf{C_A}\mathbf{A})$ obtained in stage **SE-DG** $\to$ **SE-CG**.

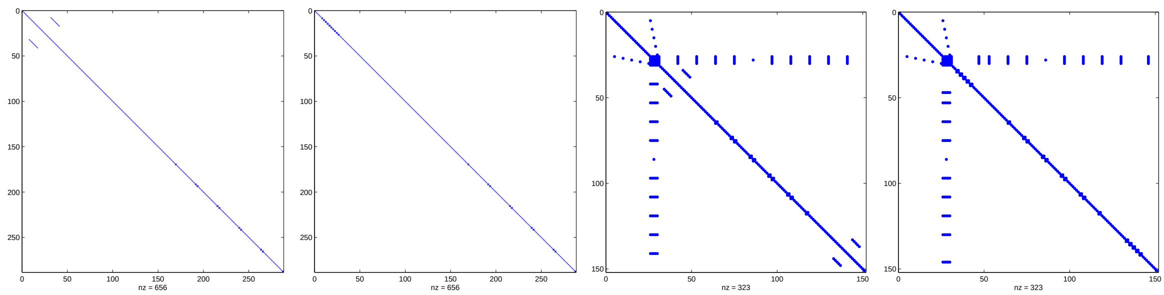

(a) before reordering (b) after reordering (c) before reordering (d) after reordering

Figure 5: Sparsity patterns for patch-inner nodal functions: (a)-(b) top left quarter of the matrix $\mathbf{B}_2$ of $p = 25$ on a single patch. (c)-(d) Matrix $\mathbf{B}_2$ on two patches with polynomial degrees 6×6 and 12×12.

Moreover, due to the mass lumping approximation involved in the definition of the bilinear form b, see (7.5) and (7.7), one can check that, given two tensorized Lagrange polynomials ϕ_ξ and $\phi_{\hat{\xi}}$ associated to LGL nodes in $\mathcal{G}_p(R)$, one has

$$b_R(\phi_\xi, \phi_{\hat{\xi}}) \neq 0 \quad \Rightarrow \quad \exists\, k, S_\ell \in \mathcal{T}_k^{(0)} \ \text{ such that } \ \xi_k, \hat{\xi}_k \in \mathcal{F}_0(I_{k,\ell_k}) \ \text{ and } \ \xi_{k'} = \hat{\xi}_{k'} \text{ for } k' \neq k. \tag{8.1}$$

In other words, there are at most three diagonals populated with nonzero entries in each of the matrices corresponding to $b_{R,1}^{(0)}$ and $b_{R,2}^{(0)}$, but the positions of the diagonals besides the main diagonal differ in both matrices.

In order to bring the non-trivial diagonals as closely together as possible we use a special ordering exploiting the fact that for C_{aspect} large enough the sets of nodes contained in $\mathcal{T}_1^{(0)}(R)$ and $\mathcal{T}_2^{(0)}(R)$, respectively, are disjoint and can each be reordered separately. More precisely, we deviate from the default line-wise ordering in the first coordinate direction only for patch-inner nodes in $\mathcal{T}_k^{(0)}(R)$, $k \neq 1$, switching to a line-wise ordering in direction k, see Fig. 6 for the details. Note that this reordering technique can still be applied for smaller C_{aspect} when there are nodal basis functions where the corresponding node is contained in $\mathcal{T}_1^{(0)}(R) \cap \mathcal{T}_2^{(0)}(R)$ as long as these basis functions do not produce an off-diagonal entry with other patch-inner basis functions in $\mathcal{T}_1^{(0)}(R) \cup \mathcal{T}_2^{(0)}(R)$, see e.g. nodes 16 and 19 in Fig. 6(b).

The resulting linear system of equations has a block-diagonal matrix of tridiagonal submatrices, see Fig. 5(b), and can be inverted in $\mathrm{O}(N)$ operations, where N is the size of $\mathbf{B}_2$.

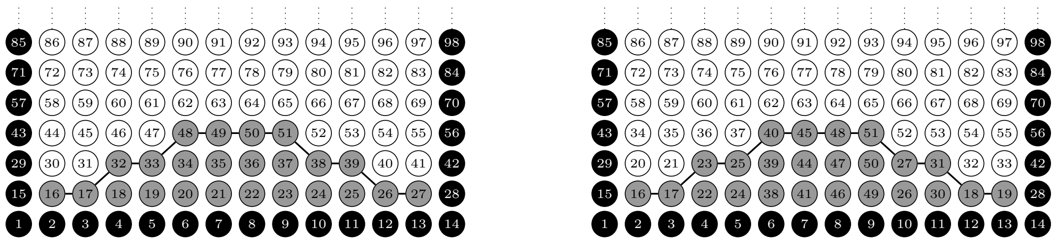

(a) Line-wise numbering. (b) Reordered numbering.

Figure 6: Schematic illustration of the numbering of the inner degrees of freedom in a single patch R of polynomial degrees 13×13 for $C_{\text{aspect}} = 1.6$. Because of the symmetry, only the lower half of the patch is shown. Black nodes: boundary degrees of freedom, gray nodes: inner degrees of freedom corresponding to vertices of cells in $\mathcal{T}_2^{(0)}(R)$, white nodes: inner degrees of freedom corresponding to vertices that are not vertices of cells in $\mathcal{T}_2^{(0)}(R)$.

Multiple patches: Gauß-Seidel relaxation on the skeleton When $\mathcal{R}$ consists of several patches, the situation is more complicated. Note that although b is defined on $\hat{V}$, it is only evaluated for piecewise polynomial functions from the space V. Due to the continuity of functions in V across cell interfaces, the matrix $\mathbf{B}_2$ in general is no longer tridiagonal as shown by Figures 5(c) and 5(d). There the sparsity pattern of the matrix $\mathbf{B}_2$ is depicted for the situation of two patches of polynomial degrees 6×6 and 12×12 which meet at a common interface. The top left part of the matrix corresponds to the degrees of freedom of the patch with lower polynomial degree, while the degrees of freedom of the patch of higher polynomial degree are represented by the lower right part. Since the trial functions are polynomials on each element R, the coupling is based on polynomial interpolation causing the additional non-zero entries off the central bands. When the polynomial degrees on both sides of an interface do not agree, every basis function on the element with lower degree corresponding to a node on the interface has to be expanded as a linear combination of higher degree Lagrange basis functions on that interface. The continuity requirement therefore causes that a lower-degree Lagrange polynomial is coupled with a linear combination of face-inner Lagrange polynomials on the higher-degree side. At a common element vertex, the coupling involves all Lagrange polynomials with reference node located on an interface containing the element vertex.

In order to solve the linear system with $\mathbf{B}_2$, we alternate a Gauß-Seidel relaxation over the skeleton of $\mathcal{R}$ and a block elimination for each $R \in \mathcal{R}$ in the spirit of substructuring methods. For the patchwise block elimination process for the bulk degrees of freedom we invoke the method detailed in the preceding paragraph.

8.3.2 Dependence on the polynomial degree

As in Sect. 8.2.3 for the first stage, we now analyze the performance of the preconditioner for the second stage. The dependence of the condition numbers of the preconditioned linear systems on the polynomial degrees is depicted in Fig. 7 for the two test cases. In all cases we choose $\alpha = 1.2$, which is a reasonable choice that balances two effects: on the one hand, the auxiliary space $\tilde{V} = V_{h,D} \cap H_0^1(\Omega)$ is rich enough for a good approximation of elements of V, on the other hand, the dimension of $\tilde{V}$ is not too high such that the linear systems of equations for the auxiliary problem is not infeasibly large.

Note that the nodes of an LGL-grid gradually move with growing polynomial degree. In contrast, due to their more rigid structure, the associated dyadic grids evolve more abruptly with occasional stagnation. This seems to cause some oscillations in constants related to the interplay between the LGL- and the associated dyadic grids, see also [10].

Furthermore we have to fix the constant C_{aspect} that limits the aspect ratios of subcells to which an inverse estimate is applied in the formation of the auxiliary form b. In the recorded numerical experiments we set $C_{\text{aspect}} = 2$. For larger C_{aspect} the condition numbers up to polynomial degree $p = 40$ exhibit a more pronounced oscillatory behavior. Although they appear to lower again after a burst of such oscillations a clear asymptotic bound cannot be observed in this range yet. As in the first stage in Subsect. 8.2.2, the tuning constant $c_{\xi,\xi'} \sim 1$ is still a free parameter. Due to the oscillations in the condition numbers, it is less clear how to find an optimal choice because we are lacking a clear objective functional. In preliminary studies we found that $c_{\xi,\xi'} = 0.6$ is a good choice which partially compensates for the effect of the constant appearing in the inverse estimate.

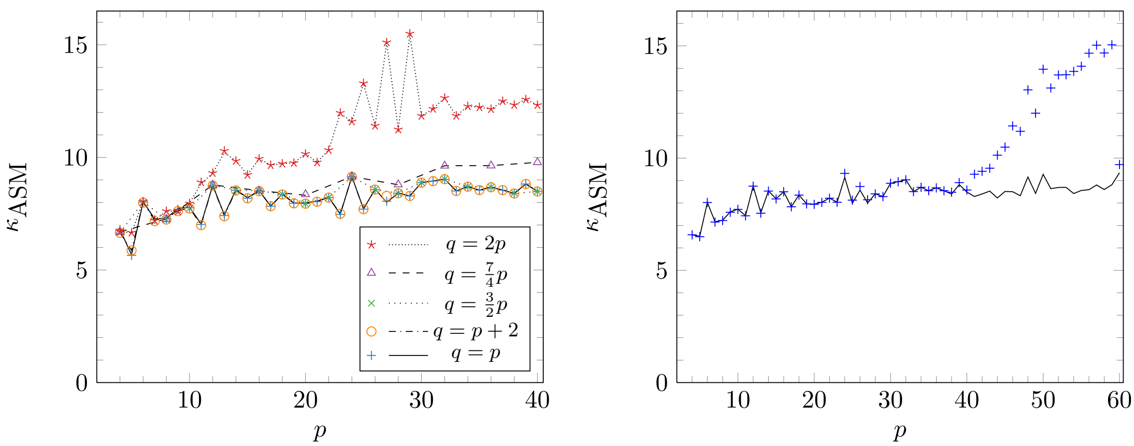

(a) First test scenario

(b) Second test scenario

Figure 7: Condition numbers $\kappa_{\text{ASM}} = \kappa(\mathbf{C_A A})$ obtained in stage **SE-CG** $\rightarrow$ **DFE-CG**.

Figures 7(a) and 7(b) show the condition numbers obtained in the second stage by the auxiliary space method in the first and second test scenario, respectively. The marked points indicate the condition numbers obtained by approximately solving the smoothing problem with the aid of 7 iterations of the substructuring method. In contrast, in both plots the continuous graphs represent the results when the smoothing problem is solved exactly using a direct method.

For the first test scenario the condition numbers are presented for p ranging from 4 to 40. In the cases (i) $q = p$, (ii) $q = p + 2$ and (iii) $q = 3/2p$ the condition numbers vary only mildly, probably due to the discrete process of dyadic grid generation. In contrast, we observe an increase of the condition numbers when larger jumps between the polynomial degrees on adjacent elements are considered according to the cases (iv) $q = 7/4p$ and, in particular, to (v) $q = 2p$. A more thorough analysis reveals that this phenomenon is caused by the slow convergence to the asymptotic limit of the constant in the estimate analogous to (7.16) for $m = 1$, where the roles of the LGL- and dyadic grids are interchanged. This estimate enters the proof of the properties of the operator $\tilde{Q}$ in Proposition 7.8 and affects the dependence of the constants in the ASM conditions (3.4) and (3.6) on the polynomial degree. This in turn causes some growth of the condition numbers for the moderate polynomial degrees under investigation. For a detailed discussion of these approximation estimates and the convergence behavior of their constants we refer to [10].

One observes enhanced oscillations when specific polynomial degrees are present in the grid, e.g. for odd polynomial degrees close to 27 which we attribute to a resonance effect between the LGL- and dyadic grids. More detailed investigations reveal that similar oscillations are also observed for some even polynomial degrees, e.g. 50. Moreover, the resonance can be shifted to nearby polynomial degrees when the parameter α, controlling the associated dyadic grids, is varied. Therefore, our tests should be viewed as a guide for favorable choices of the dyadic grid generation parameters α depending on the employed polynomial degrees.

For the second test scenario, which is perhaps more relevant for practical applications than the first one, we investigate p in the range of 4 to 60. When the smoothing problem is solved exactly, we observe that, aside from some oscillations due to the grid resonance effect, the condition numbers grow in essence mildly for small polynomial degrees and quickly tend to a limit below 10. When solving the smoothing problem only approximately by a fixed number of substructuring iterations, we observe increasing condition numbers for polynomial degrees larger than 41. This issue will be examined more closely in forthcoming work.

For instance, using $b(\cdot,\cdot)$-orthonormal polynomials on each patch R further sparsifies $\mathbf{B}_2$ significantly. Depending on the range of p, the cost of changing bases may well be offset by the positive effect on the substructuring iteration. Detailed studies of this and related issues are deferred to forthcoming work.

Of course, from a practical point of view polynomial degrees exceeding 40 significantly are rarely encountered except in pure spectral approximations on a single element when the solution is very regular, and in this case the auxiliary problem can be solved efficiently with the method presented above.

8.4 Combined stages SE-DG $\to$ SE-CG and SE-CG $\to$ DFE-CG

After studying the effects of the two stages and their numerical effects in detail, we now combine the stages **SE-DG** $\to$ **SE-CG** and **SE-CG** $\to$ **DFE-CG** by using the second stage as a preconditioner $\mathbf{C}_{\tilde{\mathbf{A}}}$ of the auxiliary problem of the first stage. The numerical results for both test scenarios showing the condition numbers obtained when the combined preconditioner is applied are depicted in Fig. 8.

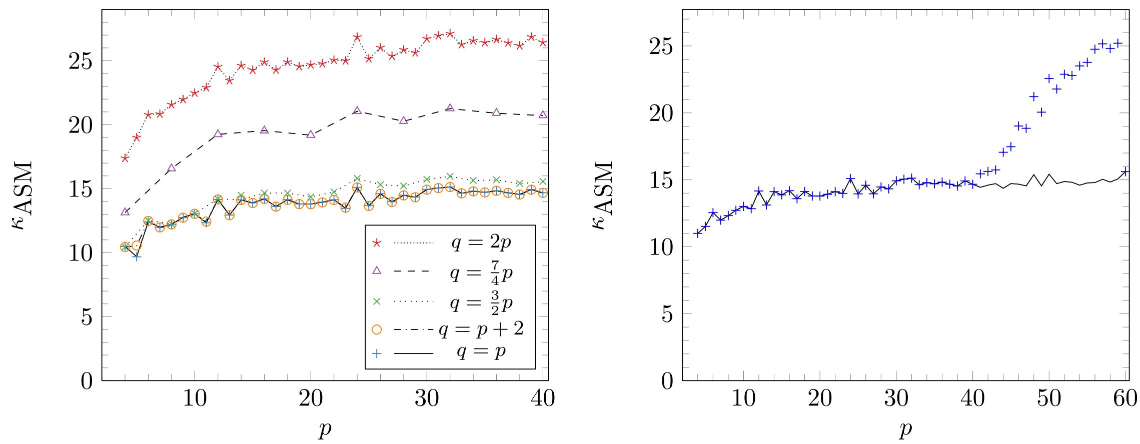

(a) First test scenario

(b) Second test scenario

Figure 8: Condition numbers $\kappa_{\mathrm{ASM}} = \kappa(\mathbf{C}_{\mathbf{A}}\mathbf{A})$ obtained in combined stages **SE-DG** $\to$ **SE-CG** and **SE-CG** $\to$ **DFE-CG**.

For both scenarios, the numerical effects observed for the single stages are also present when the combined preconditioner is used. The oscillations that have been striking in the second stage for the first scenario now only have a mild effect, but their dependence on the ratio q/p is still clearly visible. In the second scenario, for $p \leq 40$ the condition numbers for the approximate and exact solutions of the smoothing problem almost agree. For larger p the insufficiently accurate solutions of the smoothing problem by the substructuring method in the second stage lead to a deterioration of the overall condition number. When the smoothing problem in the second stage is solved exactly, the condition number is bounded by 17.

References

[1] P. Antonietti and B. Ayuso de Dios, *Schwarz domain decomposition preconditioners for discontinuous Galerkin approximations of elliptic problems: non-overlapping case.* M2AN Math. Model. Numer. Anal., 41 (2007), pp. 21–54.

[2] P. Antonietti and B. Ayuso de Dios, *Multiplicative Schwarz methods for discontinuous Galerkin approximations of elliptic problems.* M2AN Math. Model. Numer. Anal., 42 (2008), pp. 443–469.

[3] D. N. Arnold, *An interior penalty finite element method with discontinuous elements.* SIAM J. Numer. Anal., 19 (1982), pp. 742–760.

[4] D. Arnold, F. Brezzi, B. Cockburn, and L. D. Marini, *Unified analysis of discontinuous Galerkin methods for elliptic problems.* SIAM J. Numer. Anal., 39 (2002), pp. 1749–1779.

[5] Ch. Bernardi and Y. Maday, *Spectral Methods.* In: Ph. G. Ciarlet and J. L. Lions, eds., Handbook of Numerical Analysis. Vol. V, part 2, Elsevier, Amsterdam (1997), pp. 209–486.

[6] S. Beuchler, R. Schneider, and C. Schwab, *Multiresolution weighted norm equivalencies and applications.* Numer. Math., 98 (2004), pp. 67–97.

[7] S. C. Brenner, *Two-level additive Schwarz preconditioners for nonconforming finite element methods.* Math. Comput., 65 (1996), pp. 897–921.

[8] K. Brix, C. Canuto, and W. Dahmen, *Legendre-Gauß-Lobatto meshes and associated nested dyadic meshes.* IGPM preprint, RWTH Aachen, in preparation.

[9] K. Brix, *Robust preconditioners for hp-discontinuous Galerkin discretizations for elliptic problems.* Doctoral thesis. Institut für Geometrie und Praktische Mathematik, RWTH Aachen, in preparation.

[10] K. Brix, C. Canuto, and W. Dahmen, *Robust Preconditioners for DG-Discretizations with Arbitrary Polynomial Degrees.* In: Proceedings of the 21st International Conference on Domain Decomposition Methods, Rennes, France, June 25th–29th, 2012. Submitted. `arXiv:1212.6385 [math.NA]`

[11] K. Brix, M. Campos Pinto, and W. Dahmen, *A multilevel preconditioner for the interior penalty discontinuous Galerkin method.* SIAM J. Numer. Anal., 46 (2008), pp. 2742–2768.

[12] K. Brix, M. Campos Pinto, W. Dahmen, and R. Massjung, *Multilevel preconditioners for the interior penalty discontinuous Galerkin method II - Quantitative studies.* Commun. Comput. Phys., 5 (2009), pp. 296–325.

[13] C. Canuto, *Stabilization of spectral methods by finite element bubble functions.* Comput. Methods Appl. Mech. Eng., 116 (1994), pp. 13–26.

[14] C. Canuto, P. Gervasio, and A. Quarteroni, *Finite-element preconditioning of G-NI spectral methods.* SIAM J. Sci. Comput., 31 (2010), pp. 4422–4451.

[15] C. Canuto, M. Y. Hussaini, A. Quarteroni, and T. A. Zang, *Spectral methods. Fundamentals in single domains.* Springer, Berlin, 2006.

[16] C. Canuto, L. F. Pavarino, and A. B. Pieri, *BDDC preconditioners for continuous and discontinuous Galerkin methods using spectral/hp elements with variable polynomial degree.* Submitted.

[17] V.A. Dobrev, R.D. Lazarov, P.S. Vassilevski, and L.T. Zikatanov, *Two-level preconditioning of discontinuous Galerkin approximations of second-order elliptic equations.* Numer. Linear Algebra Appl., 13 (2006), pp. 753–770.

[18] J. Gopalakrishnan and G. Kanschat, *A multilevel discontinuous Galerkin method.* Numer. Math., 95 (2003), pp. 527–550.

[19] G. Kanschat, *Multilevel methods for discontinuous Galerkin FEM on locally refined meshes.* Comput. & Structures, 82 (2004), pp. 2437–2445.

[20] S. V. Nepomnyaschikh, *Fictitious components and subdomain alternating methods.* Soviet J. Numer. Anal. Math. Modelling, 5 (1990), pp. 53–68.

[21] S. V. Nepomnyaschikh, *Decomposition and fictitious domains methods for elliptic boundary value problems.* In: D. E. Keyes, T. F. Chan, G. A. Meurant, J. S. Scroggs, and R. G. Voigt, eds., Fifth International Symposium on Domain Decomposition Methods for Partial Differential Equations. Society of Industrial and Applied Mathematics, Philadelphia, 1992, pp. 62–72.

[22] P. Oswald, *Preconditioners for nonconforming discretizations.* Math. Comp., 65 (1996), pp. 923–941.

[23] S. V. Parter and E. E. Rothman, *Preconditioning Legendre spectral collocation approximations to elliptic problems.* SIAM J. Numer. Anal., 32 (1995), pp. 333–385.

[24] E. Süli, C. Schwab, and P. Houston, *hp-DGFEM for partial differential equations with nonnegative characteristic form.* In: B. Cockburn, G. E. Karniadakis, and C.-W. Shu, eds., Discontinuous Galerkin Methods: Theory, Computation and Applications. Lecture Notes in Computational Science and Engineering, vol. 11, Springer, Berlin, 2000, pp. 211–230.

[25] A. Toselli and O. Widlund, *Domain decomposition methods – Algorithms and Theory.* Springer Series in Computational Mathematics, vol. 34, Springer, Berlin, 2005.

[26] T.P. Wihler, P. Frauenfelder, and C. Schwab, *Exponential convergence of the hp-DGFEM for diffusion problems.* Comput. Math. Appl., 46 (2003), pp. 183–205.

[27] J. Xu, *Iterative methods by space decomposition and subspace correction.* SIAM Rev., 34 (1992), pp. 581–613.

[28] J. Xu, *The auxiliary space method and optimal multigrid preconditioning techniques for unstructured grids.* Computing, 56 (1996), pp. 215–235.